Lunar South Pole Boulders and Boulder Tracks: Implications for Crew and Rover Traverses

V.T. Bickel* & D.A. Kring

Human and Robotic Space Activities, NESF - July 25th, 2019

bickel@mps.mpg.de / valentin.bickel@erdw.ethz.ch

Long-Term Exploration of the Moon

High priority target is the **Lunar South Pole** and its **PSRs**:

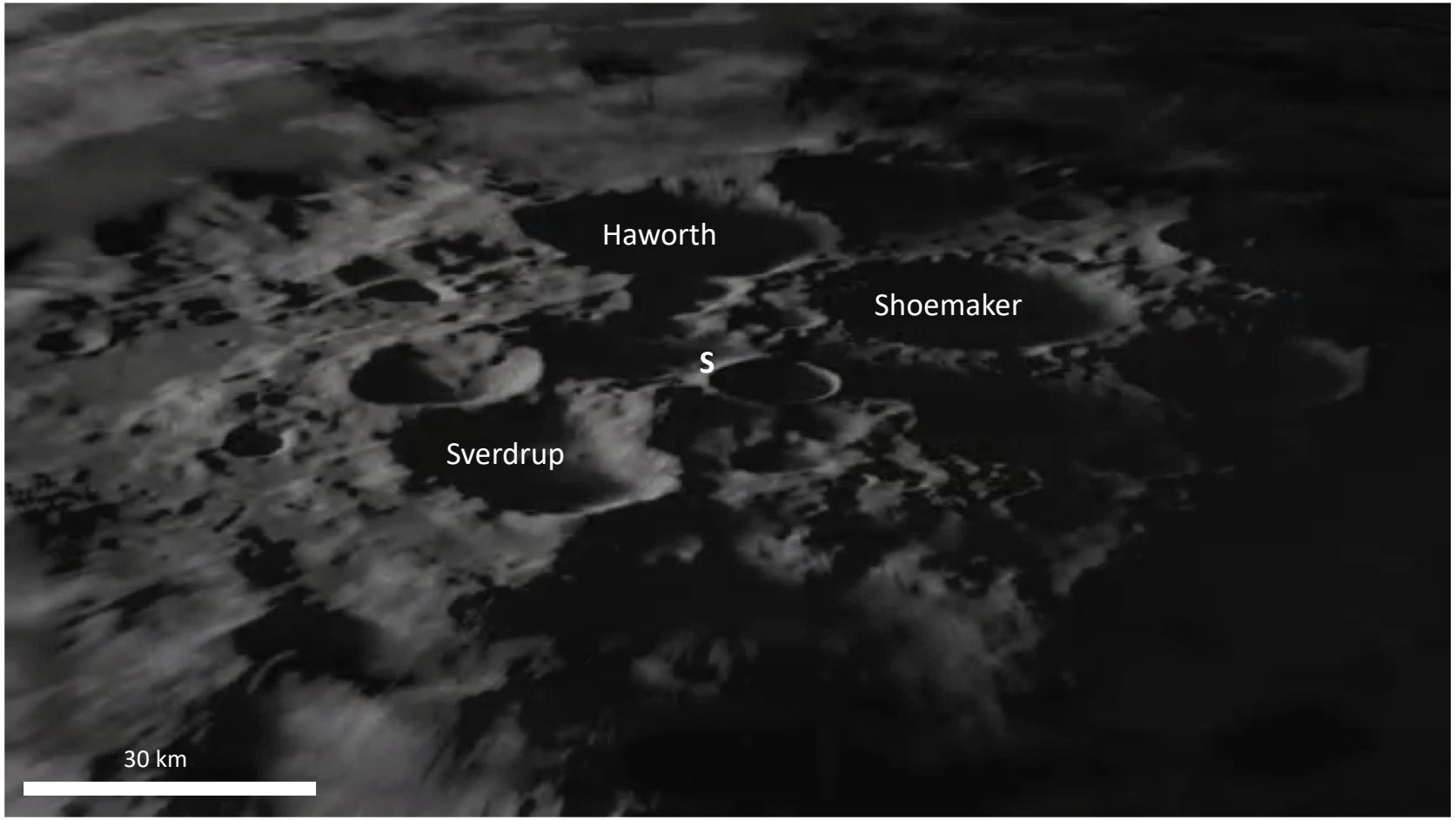

Credit: NASA Ames

Fundamental question: How trafficable is the South Pole?

What are the geomechanical properties of the South Polar regolith?

Can we derive these properties locally instead of using extrapolated Apollo/ Surveyor/ Lunokhod values?

Can we explore the polar regions with crew and robotic ground vehicles, e.g. the **Lunar Electric Rover** (LER)?

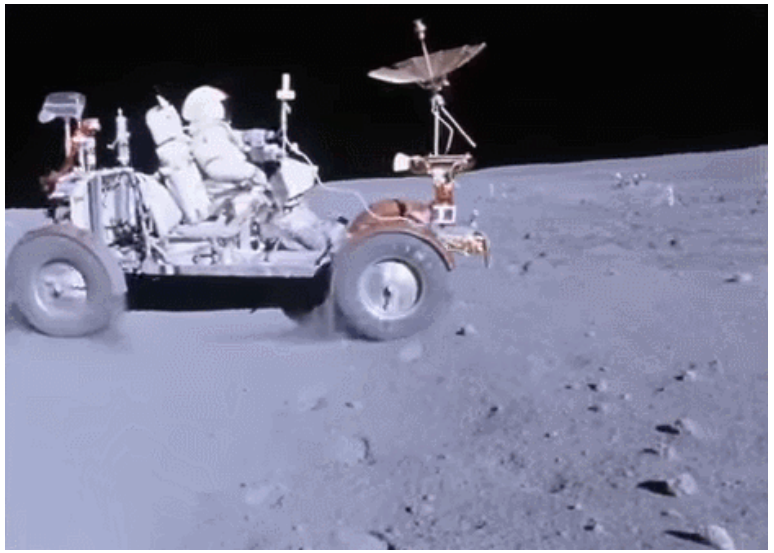

Credit: NASA

Apollo LRV - Moon

Credit: NASA JPL

Spirit MER - Mars

Rockfalls and their tracks as indicator for geomechanical properties (Bickel et al., 2019)

Detail of M138107059LC

Deep Learning-driven mapping of the South Pole

- **Neural Network** that detects rockfalls in NAC imagery (Bickel et al., 2018)

  → Poster #23

Soon available on **Moon Trek**

- **>2000 images** & **>200 Billion pixels scanned in less than one day**

- User-controlled

- **79 boulders with tracks found** from 85°S to 90°S including **58 boulders with tracks** in the **immediate vicinity** of **Shackleton crater** and the **South Pole**

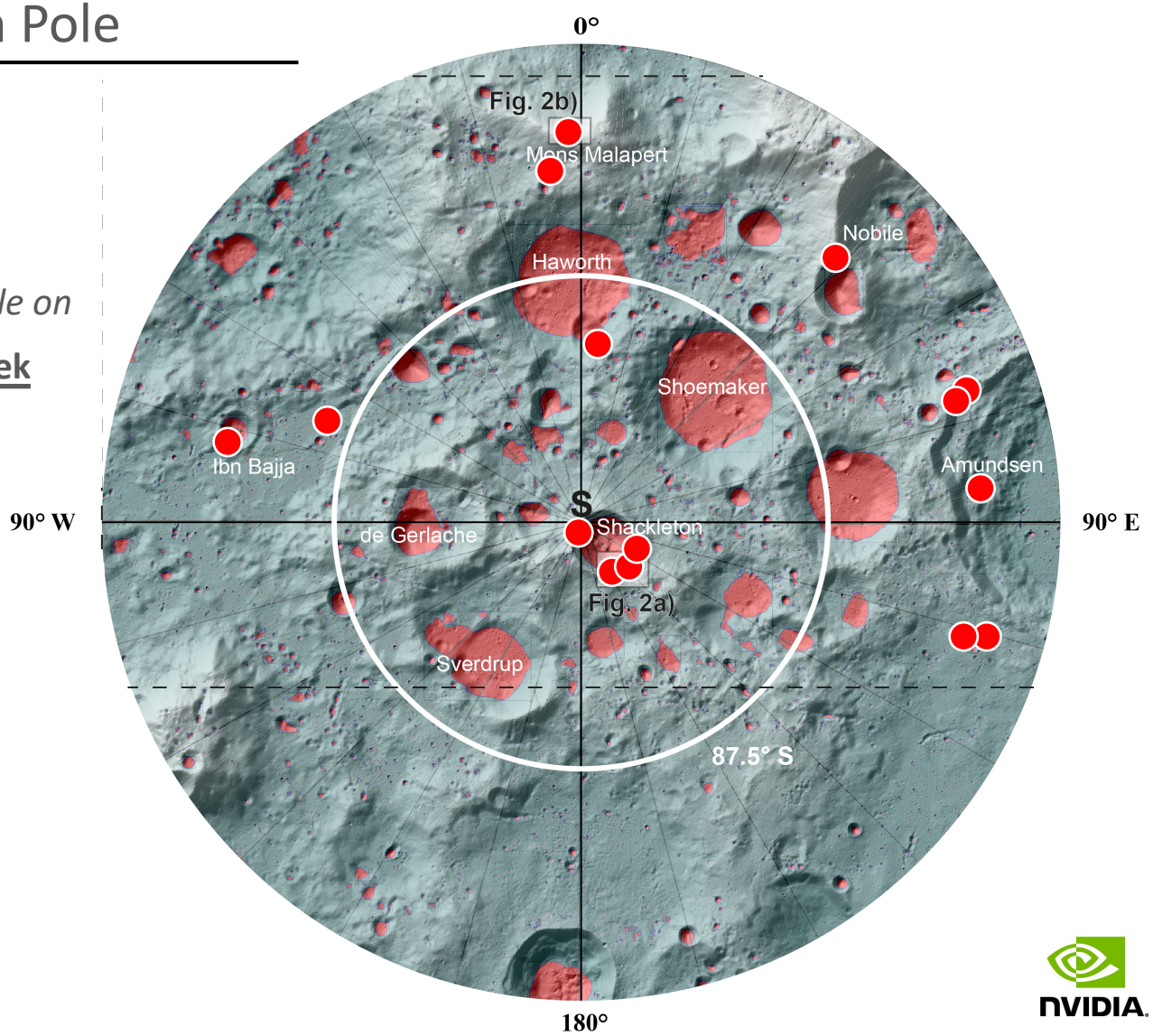

Qualitative observations of tracks

Tracks in various different lunar regions exhibit **similar track appearances**, suggesting **similar mechanical properties**:

LPD

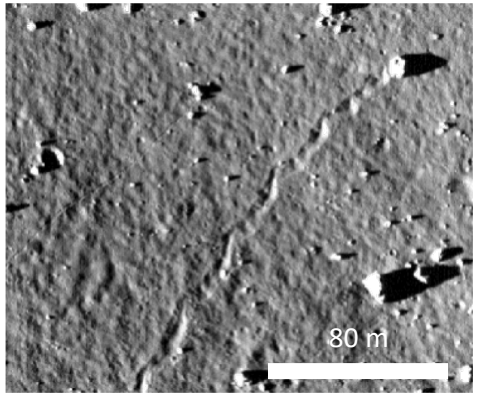

Detail of M135215829RE

Bickel et al., 2019

Mare

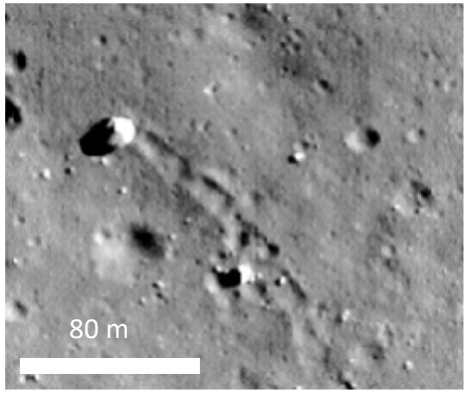

Detail of M175375107LE

South Pole

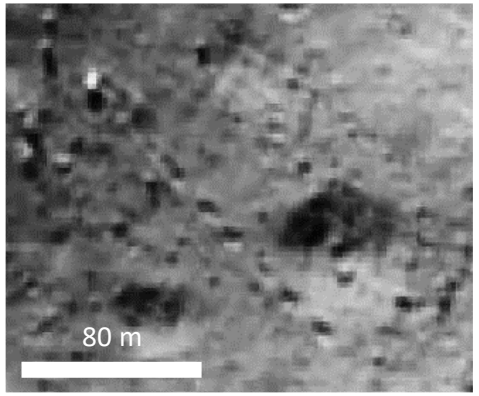

Detail of M142504842LE

Highland

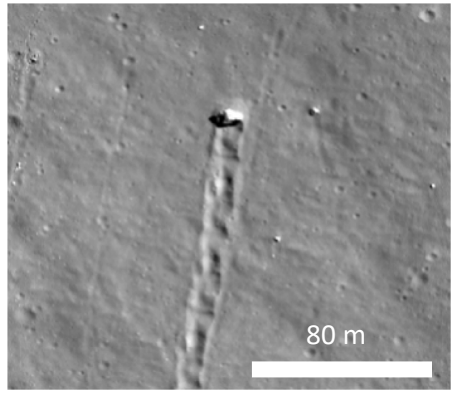

Detail of M168007359RE

Sargeant et al., 2019

PSR

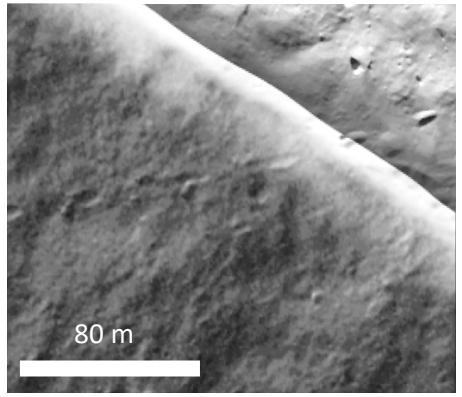

Detail of M117841678LE/RE

Quantitative determination

Static bearing capacity q_f:

Customized:
Terzaghi (1951)
Hansen (1970)

Applications:

Lander / rover sinkage
Foundations

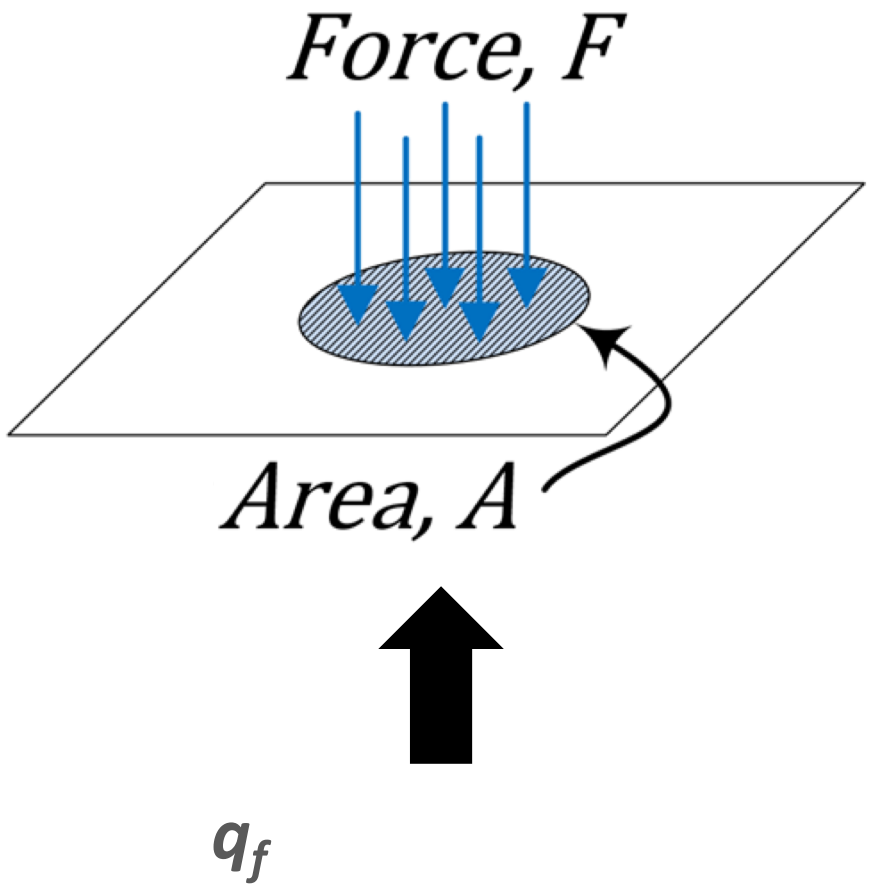

Quantitative determination

Rolling Resistance Coefficient R_{cc}:

Customized:
Carrier (1991)

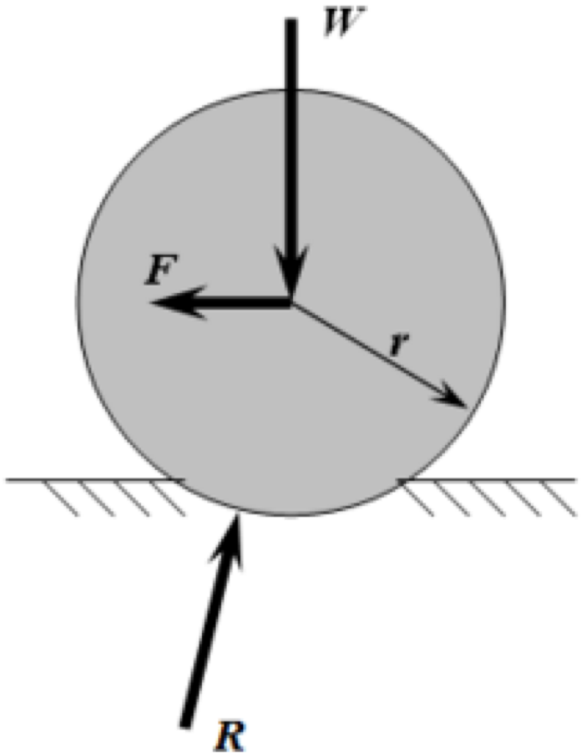

Applications:

Rover energy consumption
Rover slope climb ability

Results of quantitative analysis

South Pole bearing capacity as function of **depth**:

Bearing capacity envelope **validated** with Apollo and Lunokhod data

Bickel et al., 2019

Mean C_{rr} = 0.05

→ ~ large worn cobbles

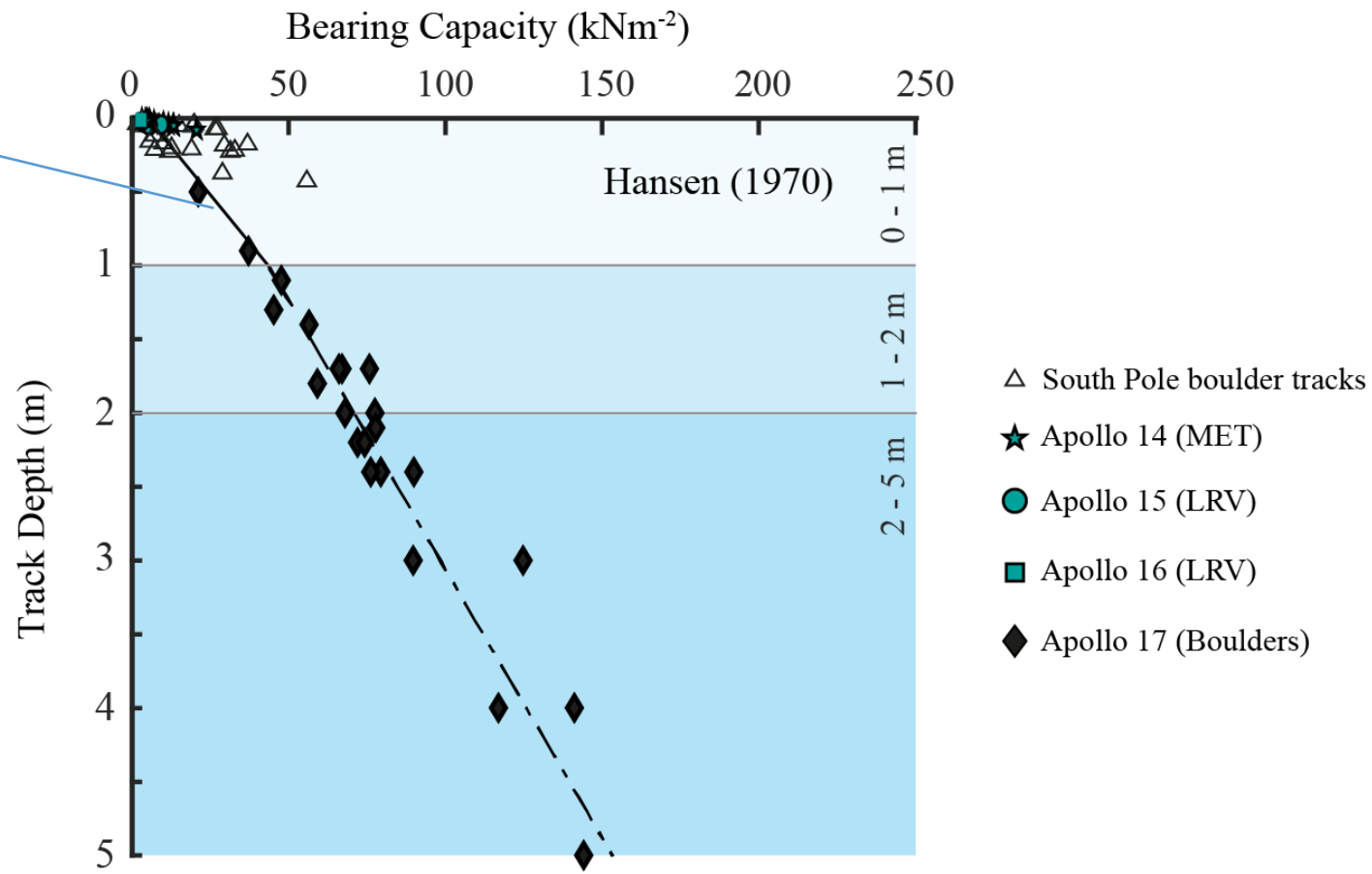

Results of quantitative analysis

Bearing capacity as function of **slope angle** (in depth range 0 to 10 cm):

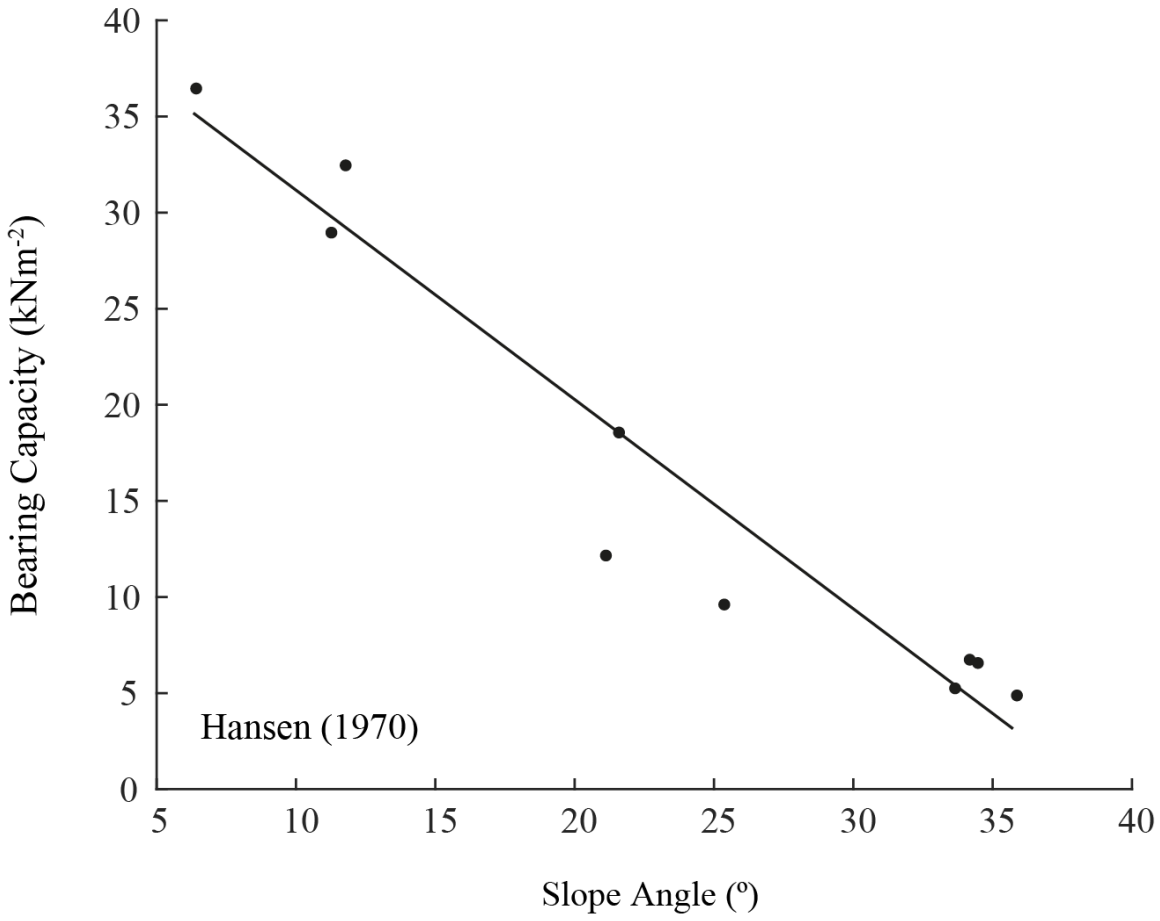

Bearing capacity as function of topography (for depth range 0 to 10 cm)

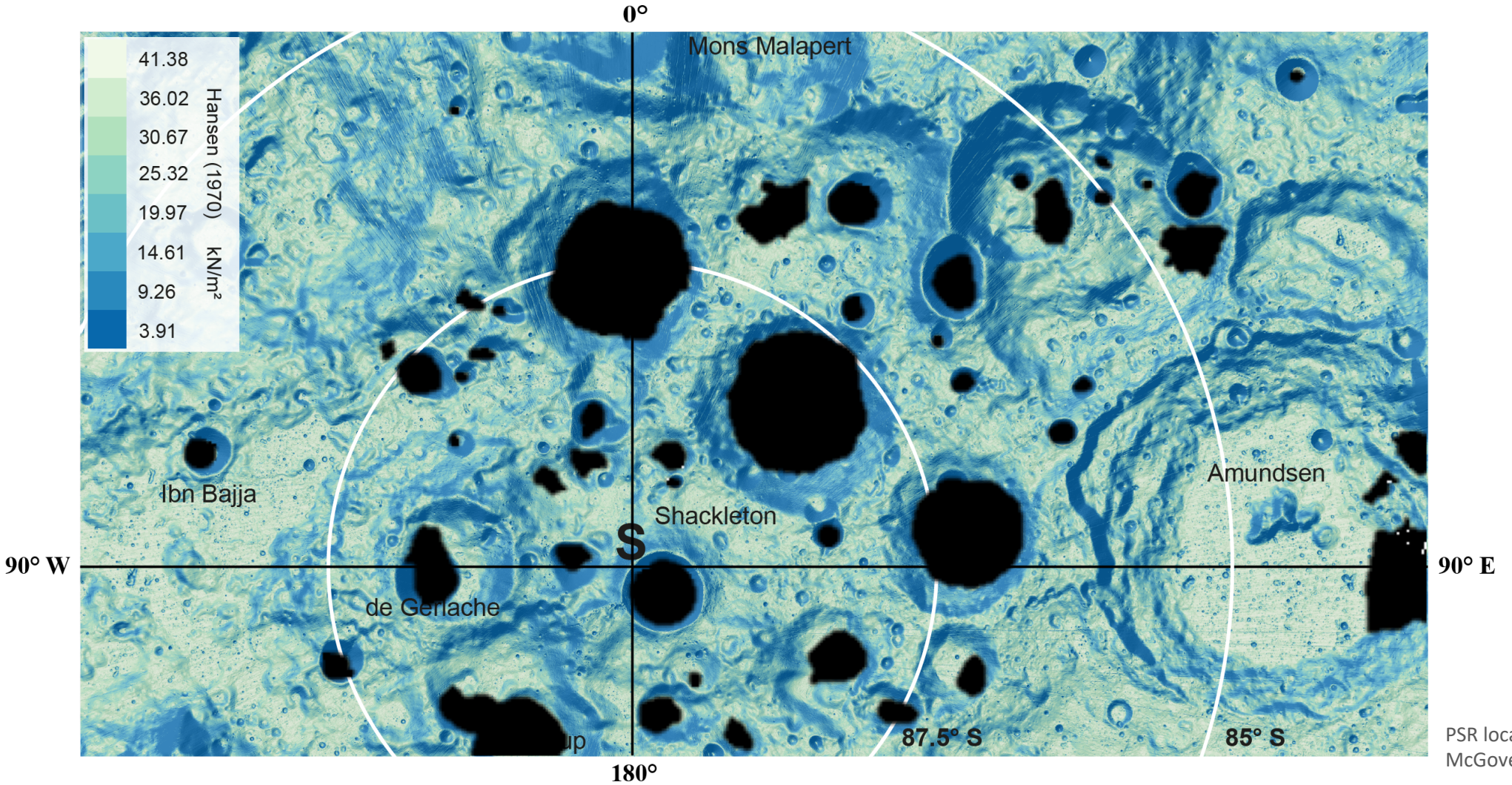

PSR locations taken from:
McGovern et al., 2013

Summary

- A **Neural Network** has been used to map 79 rockfalls at the lunar South Pole

- SP Boulder track appearance is similar to those in highland (and other) regions, **suggesting similar properties**

- SP Bearing Capacity estimates are **in line with previous studies and with in-situ observations**

  → **landers, rovers, and crew should not encounter sinkage-related issues**

- Trafficability information has been summarized in **map products** to support ongoing mission planning efforts

- **Lunar soil mechanics should be investigated in-situ** (issues in the past)

  ⇨ how can Artemis & CLPS missions help to advance our knowledge & minimize risk?

Neural Network (TGRS):

Moon Trek:

Analysis of rockfalls (JGR):

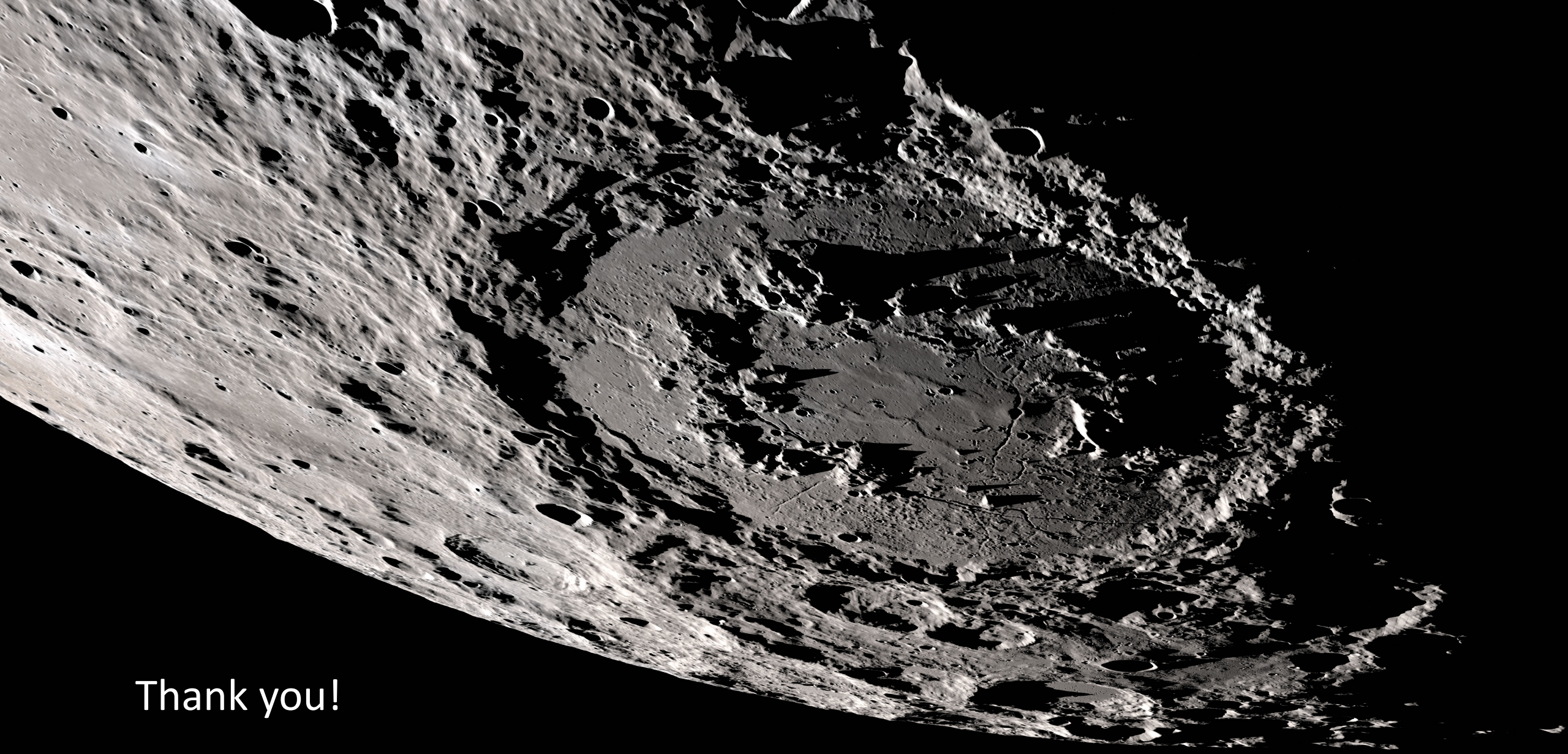

Thank you!

Credits: LPI CLSE

APOLLO 50
LUNAR AND PLANETARY INSTITUTE
NASA Johnson Space Center
Astromaterials Research & Exploration Science
Goddard SPACE FLIGHT CENTER
USRA
ARECIBO OBSERVATORY THE WILLIAM E. GORDON TELESCOPE ARECIBO PUERTO RICO 1963 - 2013
SRI
THE UNIVERSITY OF ARIZONA
UNIVERSITY of HAWAI'I MANOA
UNIVERSITY of HOUSTON
UNIVERSITY OF MARYLAND
UNIVERSITY OF NOTRE DAME

References

Bart, G. D., Nickerson, R. D., Lawder, M. T., & Melosh, H. (2011). Global survey of lunar regolith depths from LROC images. Icarus, 215(2), 485-490.

Bickel, V. T., Honniball, C. I., Martinez, S. N., …, Kring, D. A. (2019). Analysis of Lunar Boulder Tracks: Implications for Trafficability of Pyroclastic Deposits. Journal of Geophysical Research: Planets, 10.2019.

Bickel, V. T., Lanaras, C., Manconi, A., Loew, S., Mall, U. (2018). Automated Detection of Lunar Rockfalls using a Convolutional Neural Network. IEEE Transactions on Remote Sensing and Geoscience, 57(6).

Carrier, W. III, Olhoeft, G. R., & Mendell, W. (1991). Physical properties of the lunar surface. In In the Lunar Source Book, Chapter 9 (pp. 475–594). Cambridge University Press.

Fa, W., & Jin, Y. (2010). A primary analysis of microwave brightness temperature of lunar surface from Chang-E 1 multi-channel radiometer observation and inversion of regolith layer thickness. Icarus, 207, pp. 605-615.

Hansen, J. B. (1970). A revised and extended formula for bearing capacity.

Liu, C., & Evett, J. B. (1992). Soils and Foundations. Prentice Hall International.

McGovern, J. A., Bussey, D. B., Greenhagen, B. T., Paige, D. A., Cahill, J. T., & Spudis, P. D. (2013). Mapping and characterization of non-polar permanent shadows on the lunar surface. Icarus, 223(1), 566-581.

Melosh, H. J. (2011). Planetary Surface Processes. Cambridge University Press. ISBN: 9780511977848.

Mitchell, J., Bromwell, L., Carrier III, W., Costes, N., Houston, W., & Scott, R. (1972a). Soil mechanics experiment. In Apollo 15 Preliminary Science Report (Vol. 289, pp. 7.1-7.28).

Mitchell, J., Houston, W., Scott, R., Costes, N., Carrier III, W., & Bromwell, L. (1972b). Mechanical properties of lunar soil: Density, porosity, cohesion and angle of internal friction. Paper presented at the Lunar and Planetary Science Conference Proceedings.

Oberbeck, V. R., & Quaide, W. L. (1968). Genetic implications of lunar regolith thickness variations. Icarus, 9, pp. 446–465.

Sargeant, H. M., Bickel, V. T., Honniball, C. I., …, Kring, D. A. (2019). DETERMINING THE BEARING CAPACITY OF PERMANENTLY SHADOWED REGIONS OF THE MOON USING BOULDER TRACKS. LPSC 50th, Houston, TX, USA.

Scott, R., Carrier III, W., Costes, N., & Mitchell, J. (1971). Apollo 12 soil mechanics investigation. Geotechnique, 21(1), 1-14.

Shuratov, Y. G., & Bondarenko, N. V. (2001). Regolith Layer Thickness Mapping of the Moon by Radar and Optical Data. Icarus, 149(2), pp. 329-338.

Terzaghi, K. (1951). Theoretical soil mechanics: Chapman And Hall, Limited.; London.

- Previous work by Bickel et al., 2018, in IEEE Transactions on Geosciences and Remote Sensing

Bickel et al., 2018

- Single-stage object detector (RetinaNet)
- trained with ~9000 original images, augmented to > 1.2 million images during training
- CNN is scale and rotation invariant

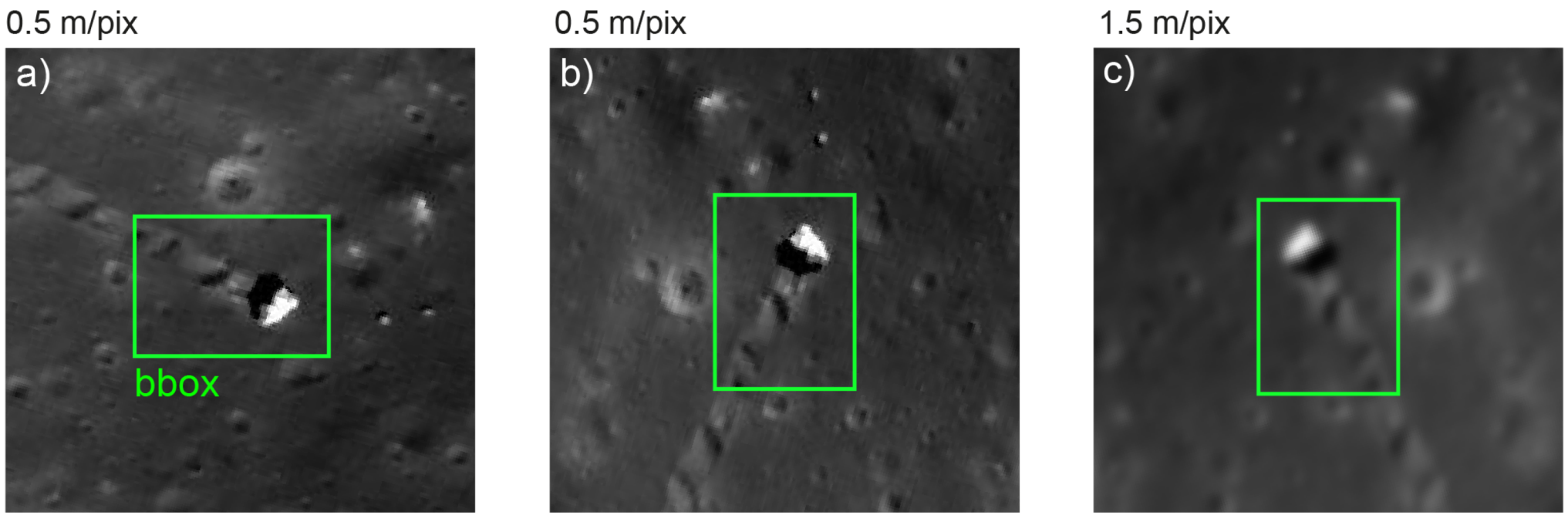

1. CNN determines the location of rockfalls on the surface of the Moon

2. CNN estimates the diameter of each mapped rockfall (boulder)

	CT	AP_{10}	$Recall_{10}$	$Precision_{10}$	AP_{25}	$Recall_{25}$	$Precision_{25}$	AP_{50}	$Recall_{50}$	$Precision_{50}$
RetinaNet (ResNet50)	**0.2**	**0.89**	**0.98**	**0.45**	0.84	0.96	0.35	0.69	0.88	0.25
	0.3		**0.90**	**0.63**		0.88	0.54		0.82	0.35
	0.4		**0.77**	**0.86**		0.77	0.84		0.75	0.60
	0.5		**0.69**	**0.98**		0.69	0.95		0.65	0.79
	0.6		**0.44**	**1**		0.44	0.96		0.39	0.85

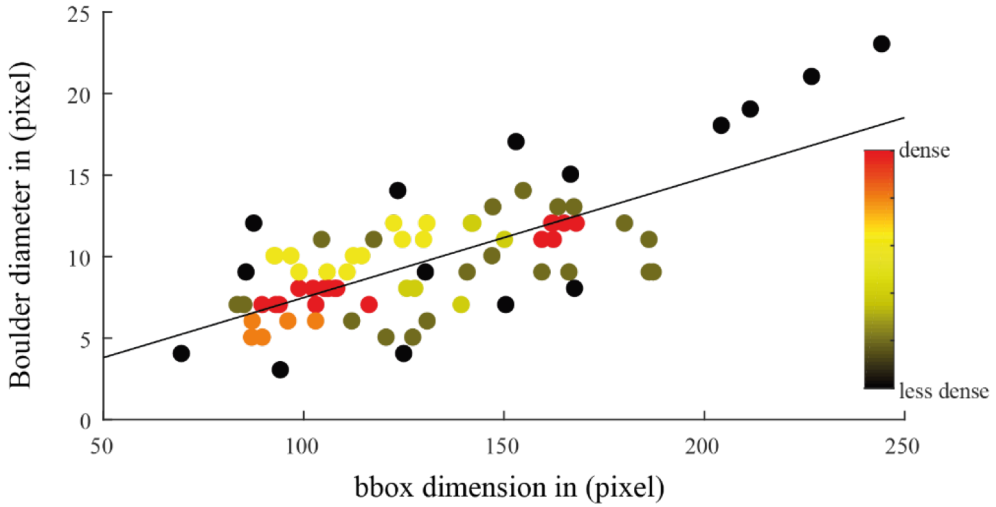

CNN performance is almost independent from NAC resolution and lighting conditions (TP, true positive):

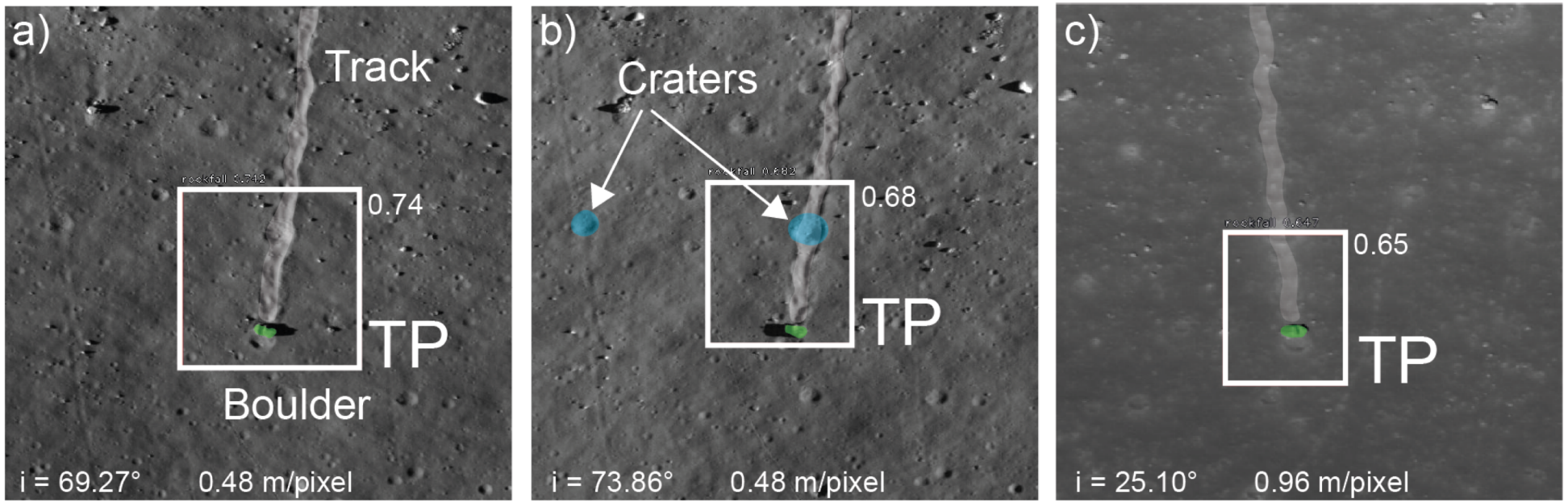

Sun EW, high res

Sun WE, high res

Sun nadir, low res

Extreme image geometry and lighting conditions cause detection issues (FN & FP, false negatives & false positives):

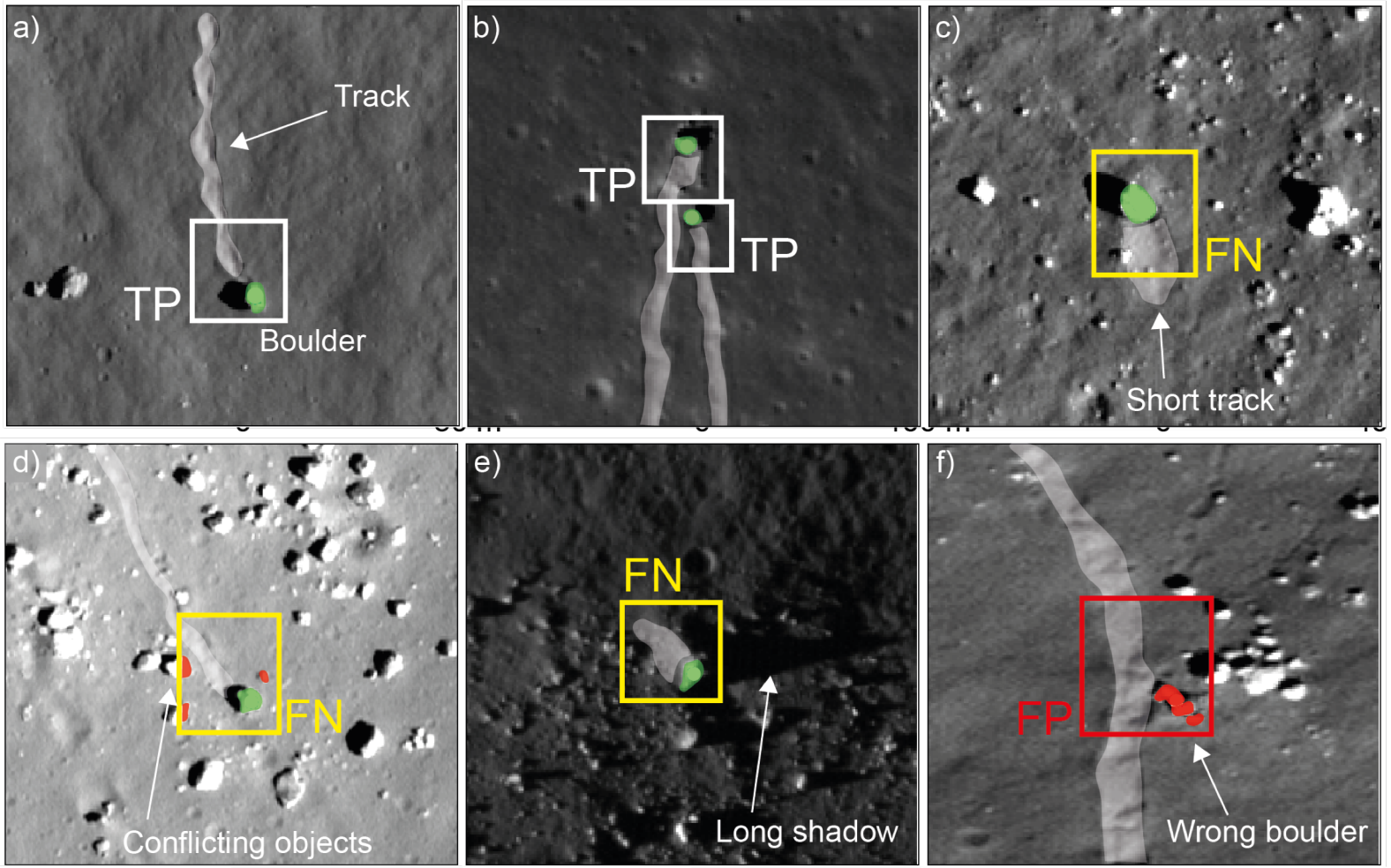

CNN detections are used for network re-training to improve performance over time:

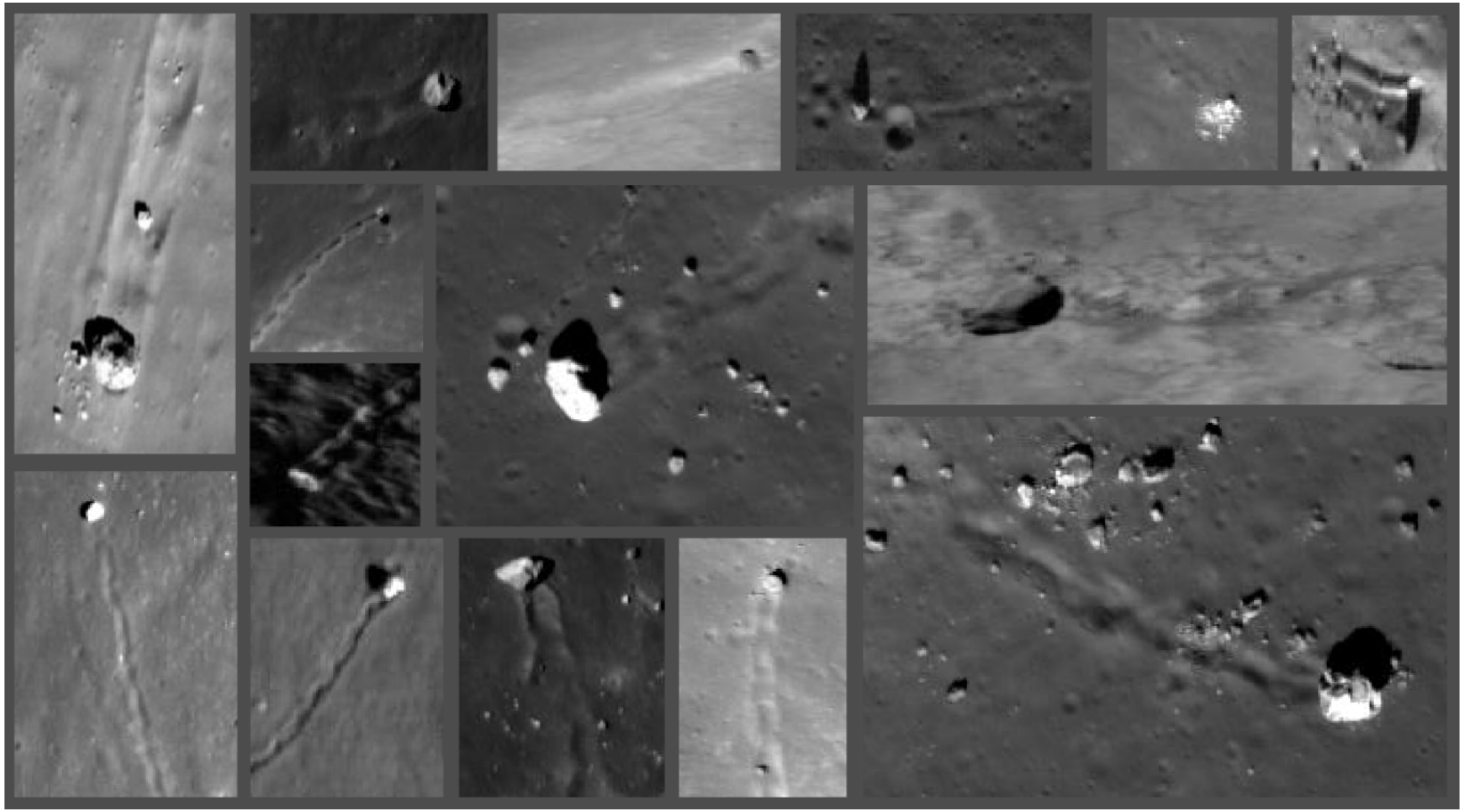

Example detections: various sizes, albedo, track shapes, illumination, etc.

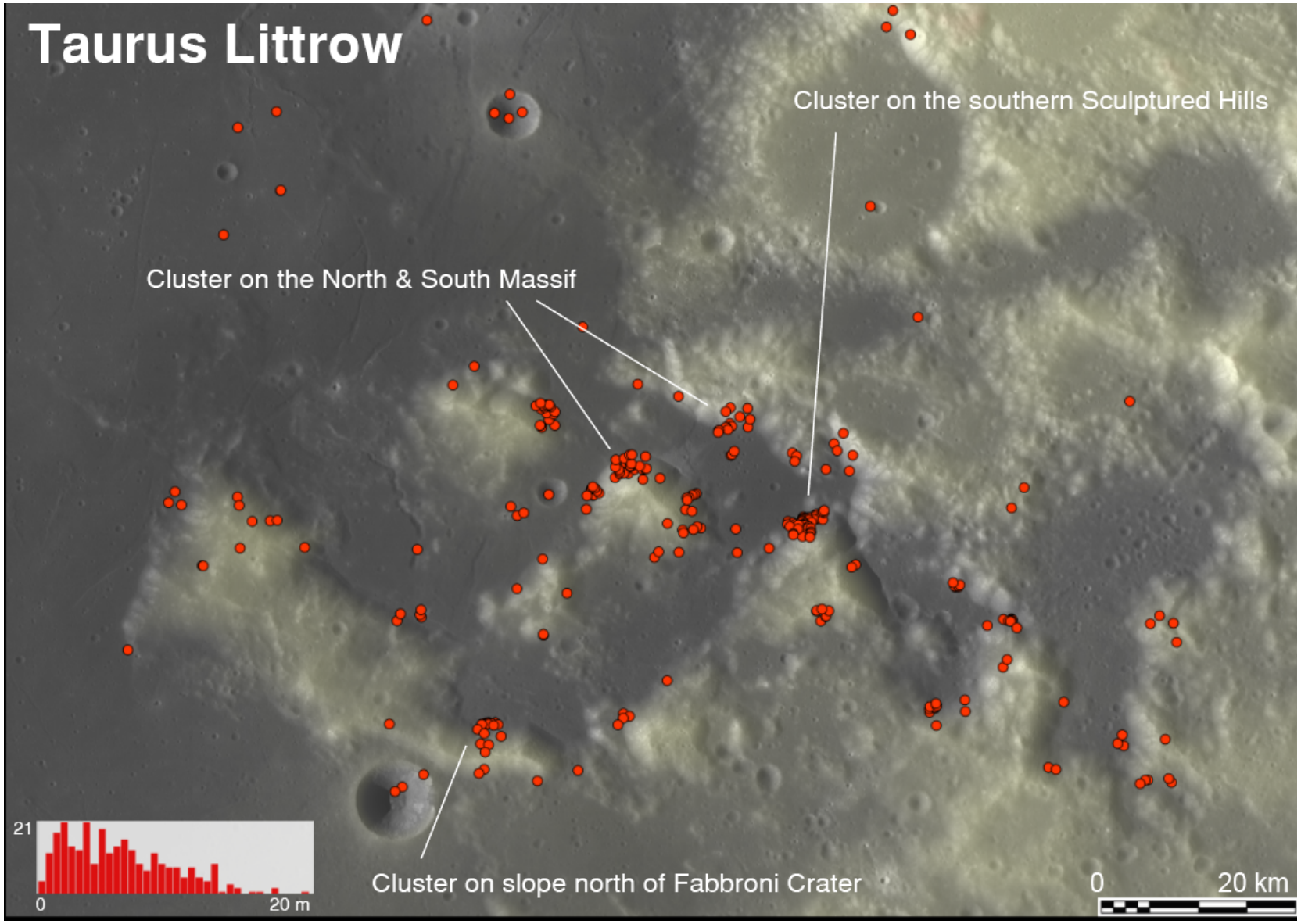
Taurus Littrow
Cluster on the southern Sculptured Hills
Cluster on the North & South Massif
Cluster on slope north of Fabbroni Crater
21
0
20 m
0
20 km

South Pole Boulders

Shackleton Crater

First landing site?

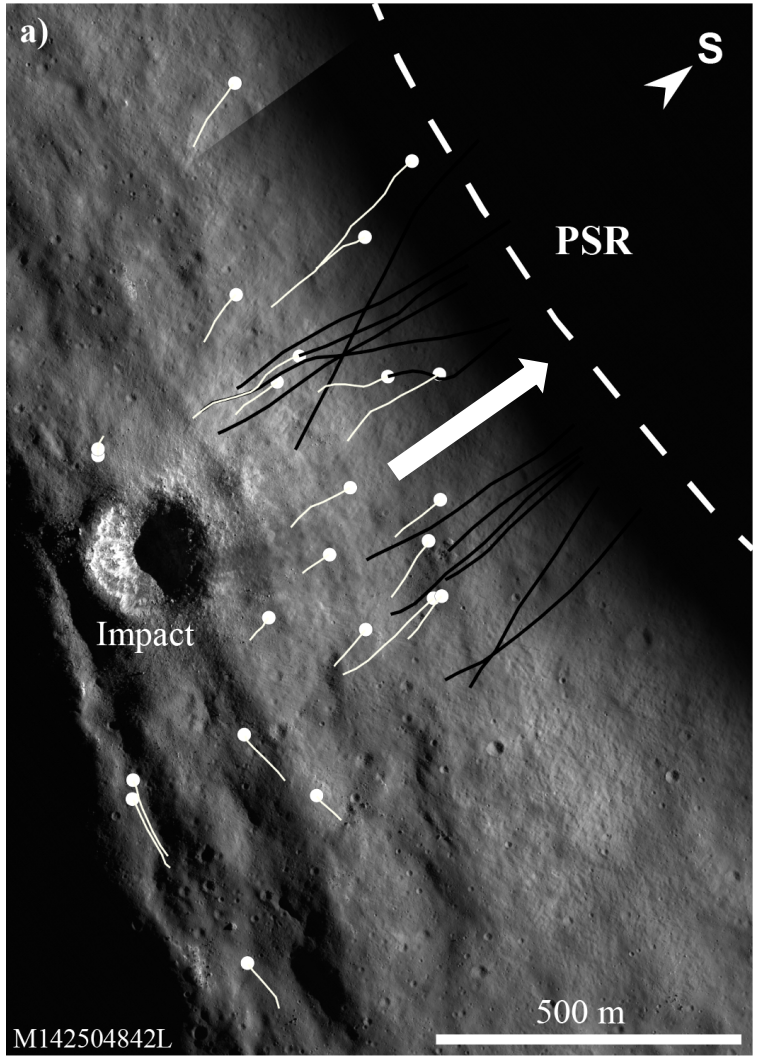

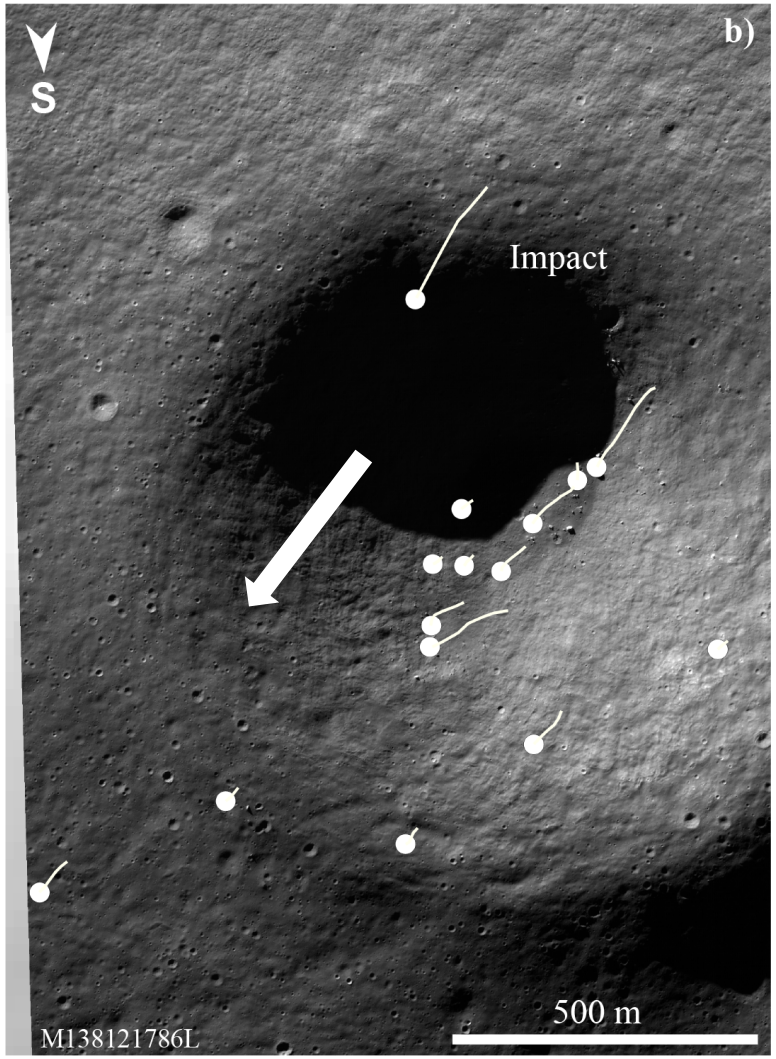

Mons Malapert

Permanent structures?

South Pole Boulders

- South Pole rockfalls are smaller
- ~ are rounder
- ~ occur on steeper slopes
- ~ have shallower tracks
- ~ have shorter runouts

Observations might be biased by the illumination conditions & topography

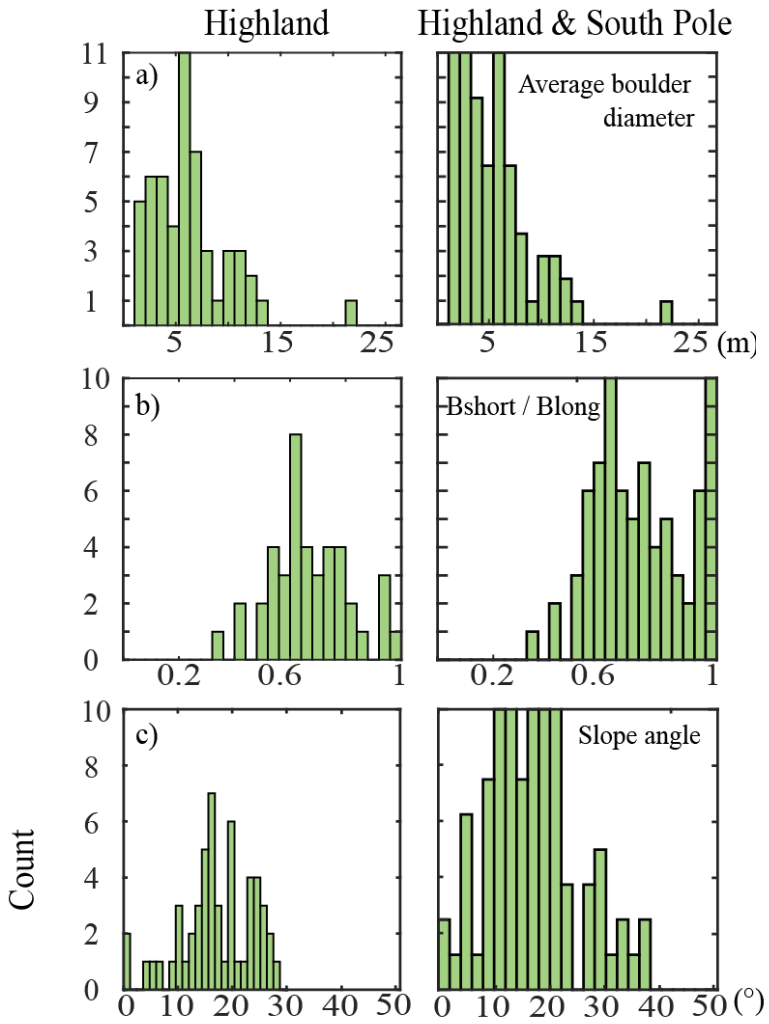

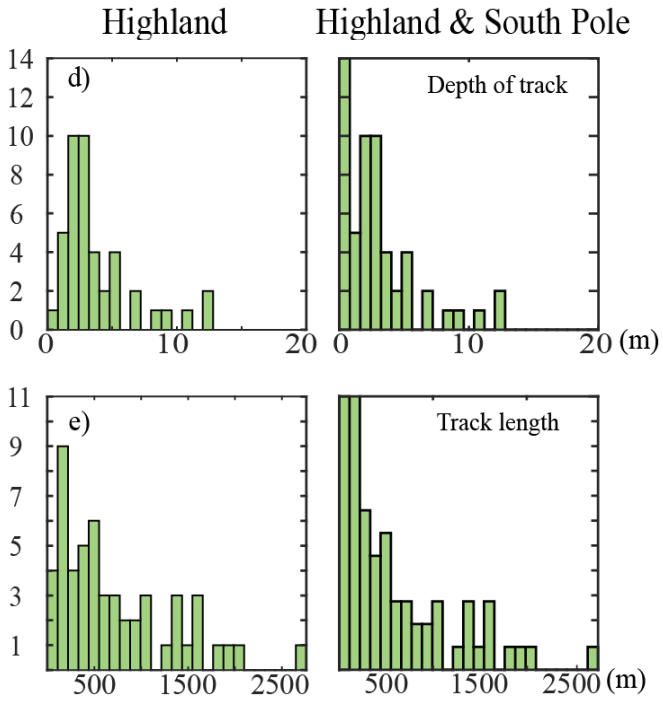

Quantitative determination

Static bearing capacity q_f:

Terzaghi (1948)

$$q_f = \underbrace{1.3cN_c}_{\text{Cohesion}} + \underbrace{q_0 N_q}_{\text{Surcharge}} + \underbrace{0.3\gamma_s B_{av} N_\gamma}_{\text{Friction}}$$

Hansen (1970)

$$q_f = \underbrace{cN_c s_c d_c i_c b_c g_c}_{\text{Cohesion}} + \underbrace{q_o N_q s_q d_q i_q b_q g_q}_{\text{Surcharge}} + \underbrace{0.5\gamma B_H N_\gamma s_\gamma d_\gamma i_\gamma b_\gamma g_\gamma}_{\text{Friction}}$$

<u>Most relevant input</u>:

- **Density**
- **Internal friction angle**
- **Boulder / Track dimensions**

Quantitative determination

Coefficient of Rolling Resistance C_{rr}:

$$C_{rr(R_c,m,g,\beta)} = \frac{R_c}{m * g * \cos\beta}$$

Carrier (1991)

$$R_c = \left(\frac{b*k}{n+1}\right) * z^{n+1}$$

Carrier (1991)

$$k = \frac{\frac{m*g}{\pi\left(\frac{b}{2}\right)^2}}{d}$$

(k coefficient of subgrade reaction, related to bearing capacity)

(n exponent of soil deformation)

Terzaghi

Terzaghi (1948) Assumptions

- Circular flat footing
- Boulder and track are on flat terrain
- Static load assumption

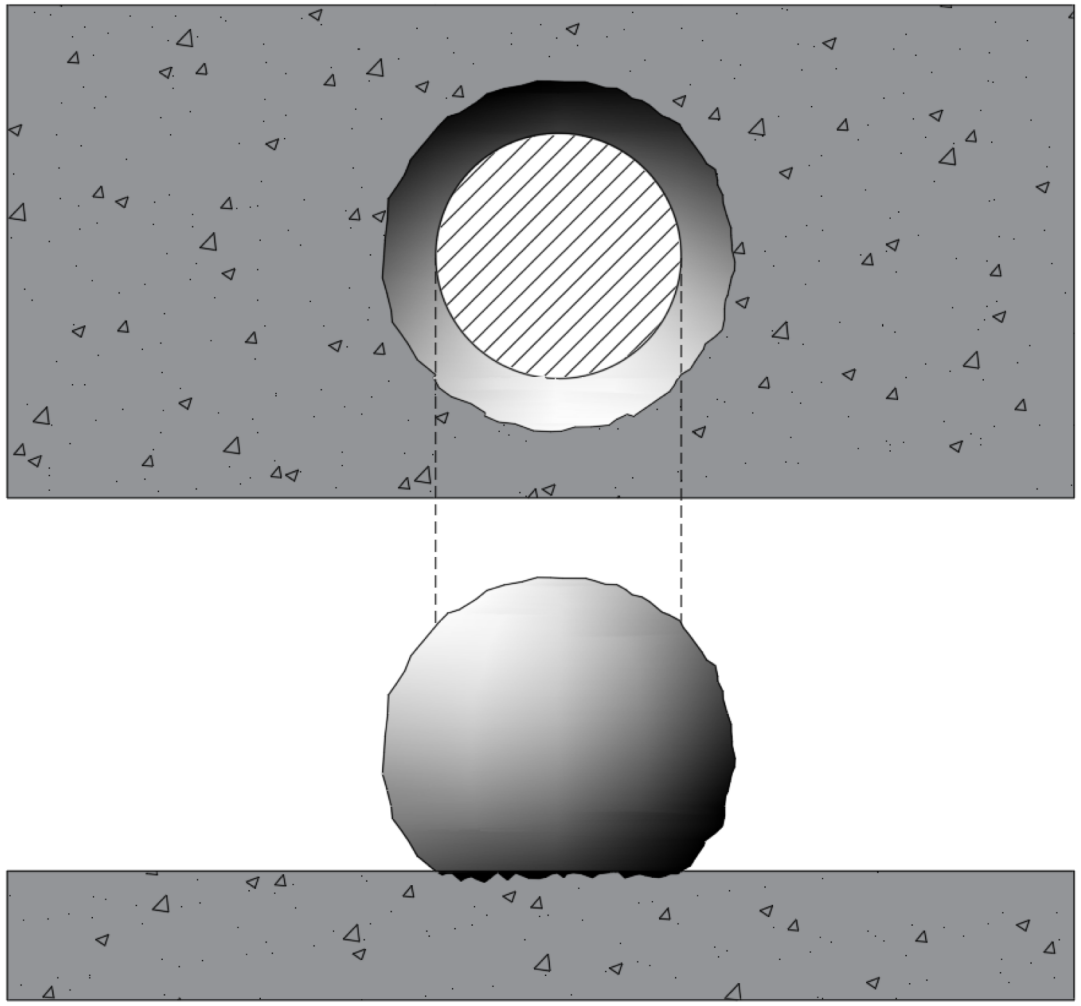

Hansen

Hansen (1970) Assumptions

- Rectangular surface
- Load and footing inclination values i and b are neglected

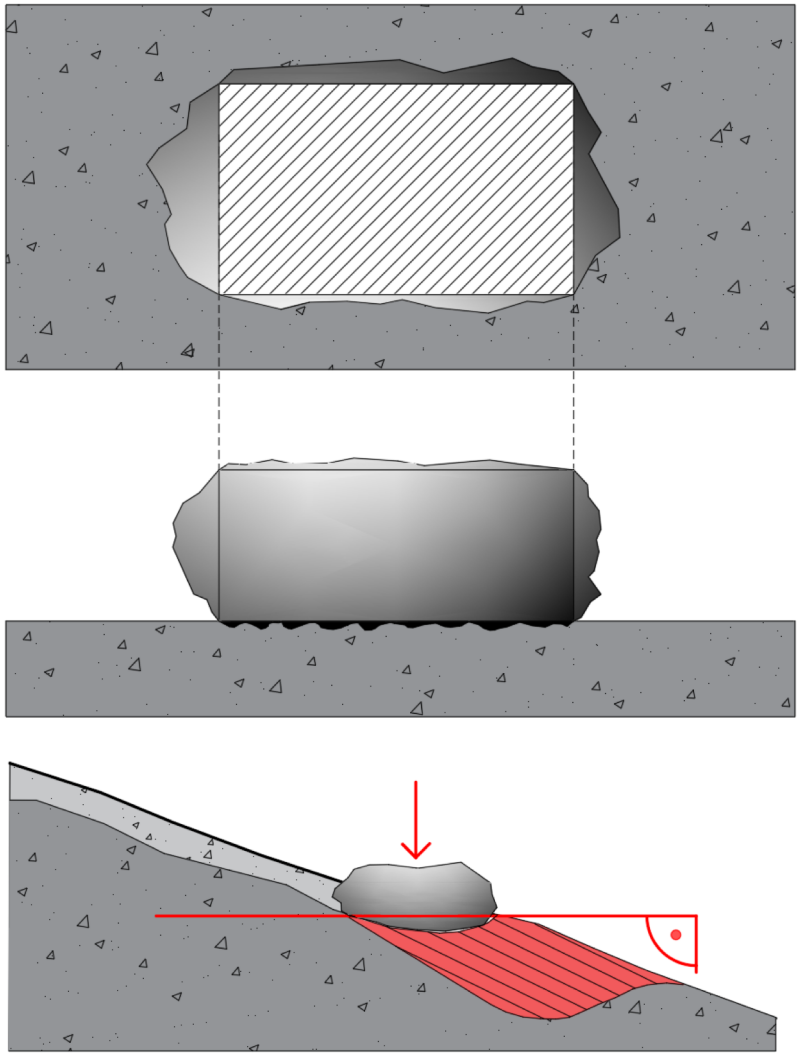

Boulder / Track dimensions

Measurement in NAC imagery:

Map view

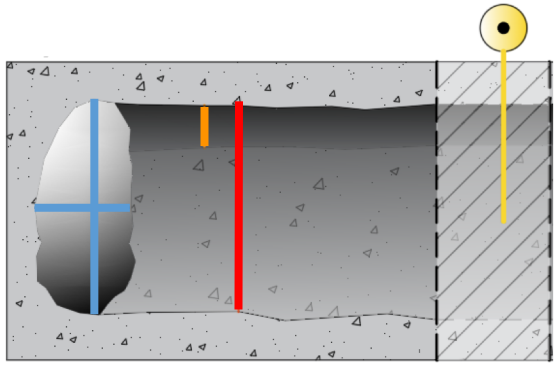

Detail of M175375107LE

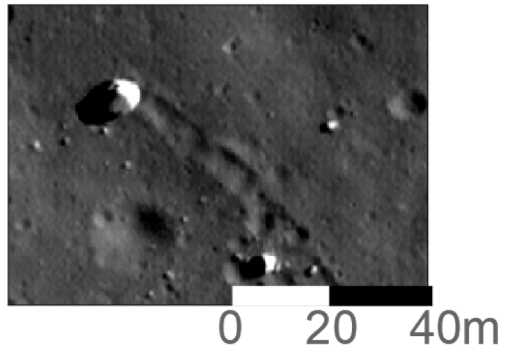

- Boulder long and short diameter
- Track width
- Shadow length

Cross Section of track

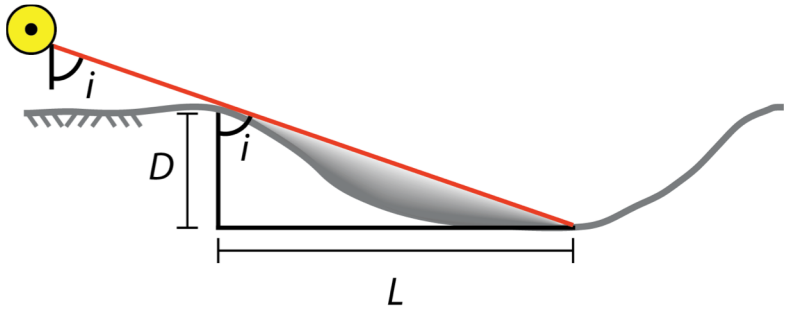

Measurements

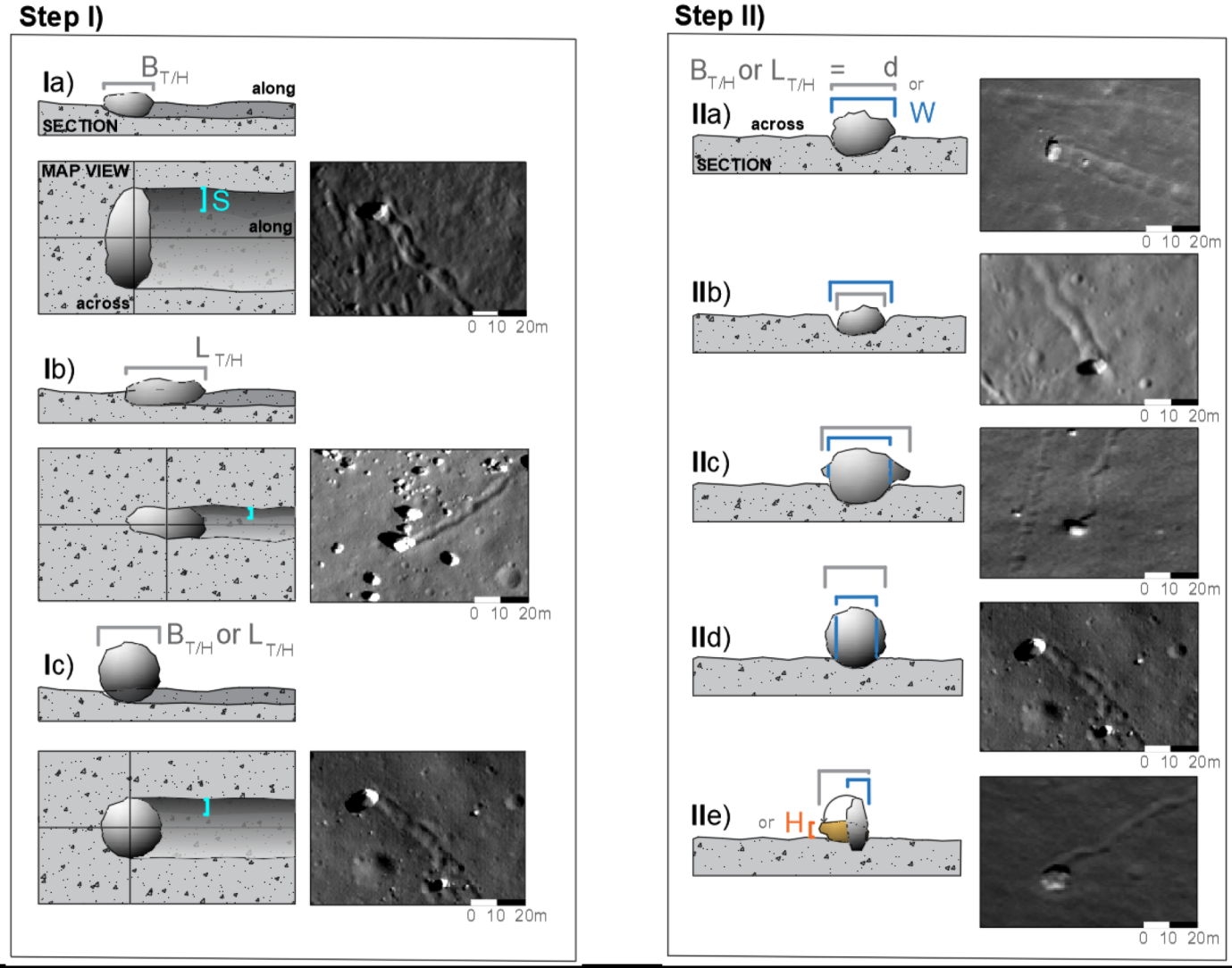

Limitations

Resolvable depth of track is dependent on spatial resolution of the used sensor (LRO NAC) = ~0.5 m/pixel:

→ shallowest measured tracks are ~**0.10 m** deep

→ **there is a sampling gap between the surface and this depth**

Additional challenge:

Large incidence angles could potentially cause errors

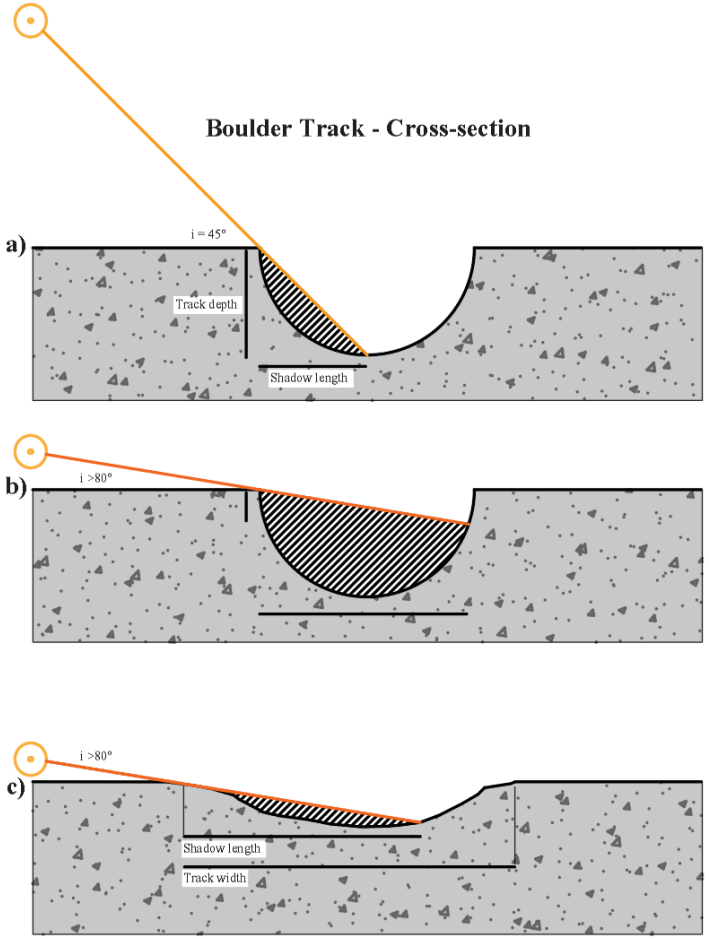

Density

Soil density values are selected from Apollo core tube analysis that best represent pyroclastic, highland, and mare material:

Terrain	Sample #	ρ (g/cm^3) Literature values*	ρ (g/cm^3) Value used
Pyroclastic	15010	1.79-1.91[a]	**1.85**
Highland/ South Pole	64001	1.66[b]	**1.66**
Mare	12025	1.96[c]	**1.96**

→ Highland values have been used as approximation for SP & PSR material

a, Mitchell et al., 1972a (Apollo 15 preliminary report)
b, Mitchell et al., 1972b (Apollo 16 preliminary report)
c, Scott, 1971
* Density values for 30 - 60 cm

Map fusion for Future Exploration

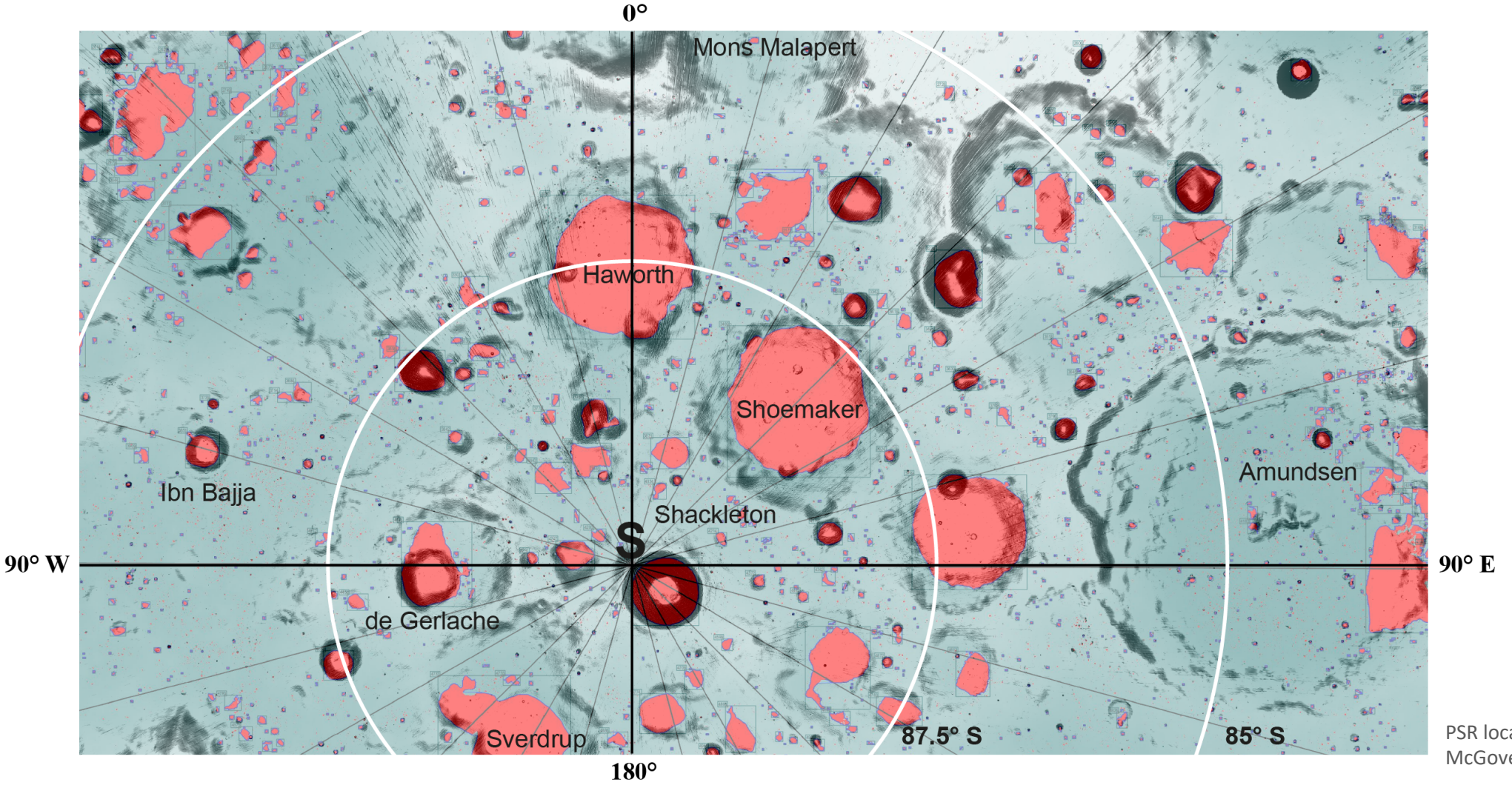

PSR locations taken from:
McGovern et al., 2013

DEMs

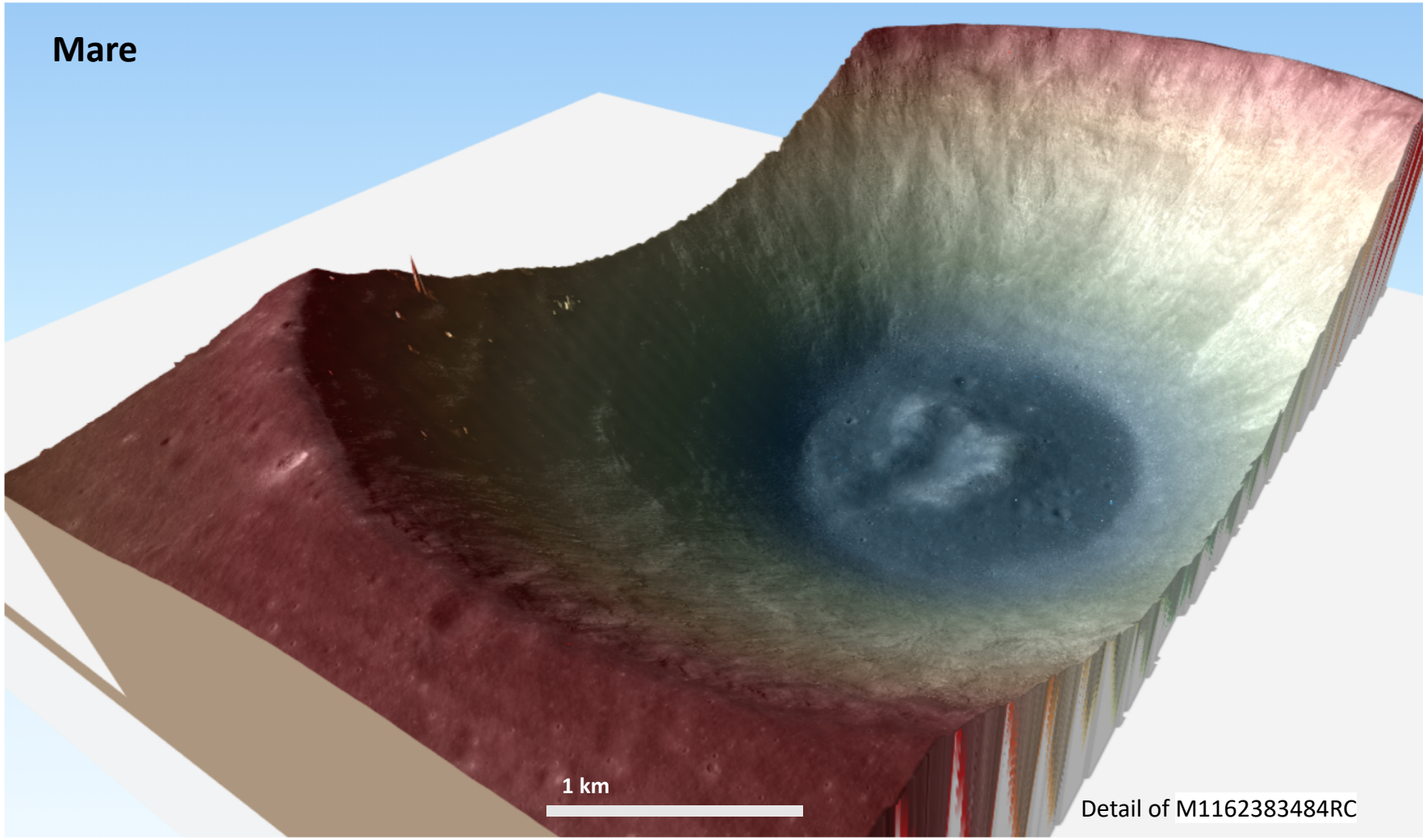

DEMs

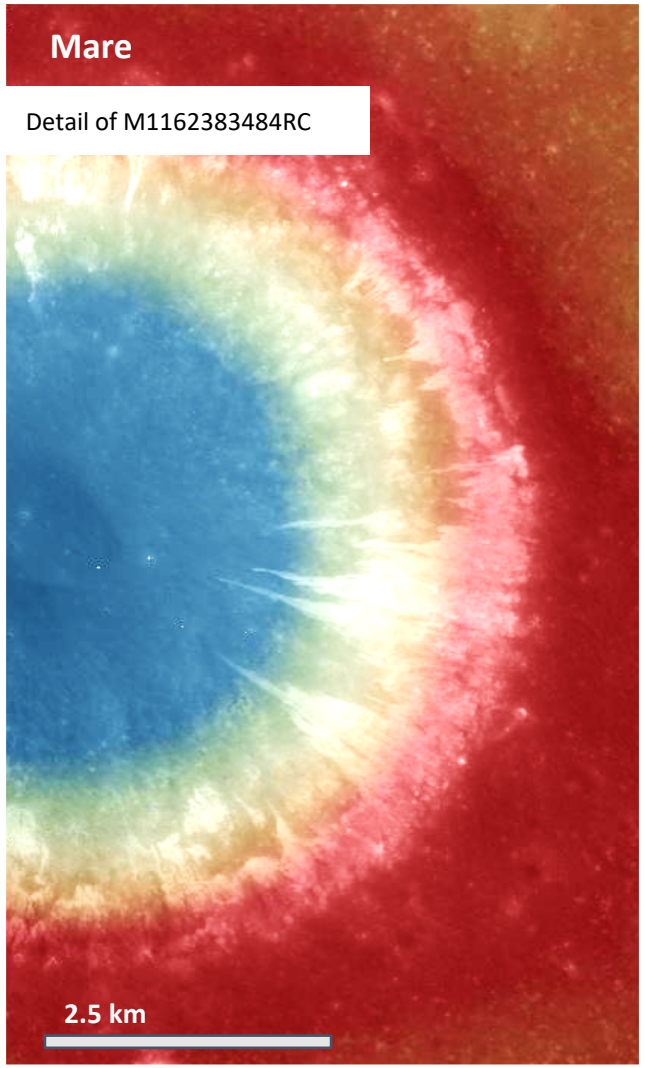
Mare
Detail of M1162383484RC
2.5 km

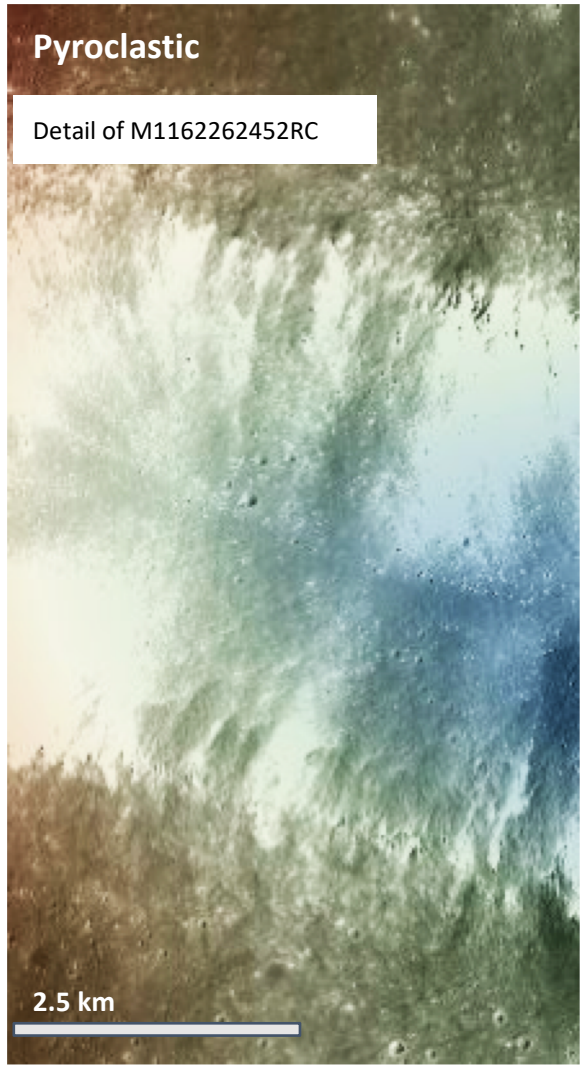
Pyroclastic
Detail of M1162262452RC
2.5 km

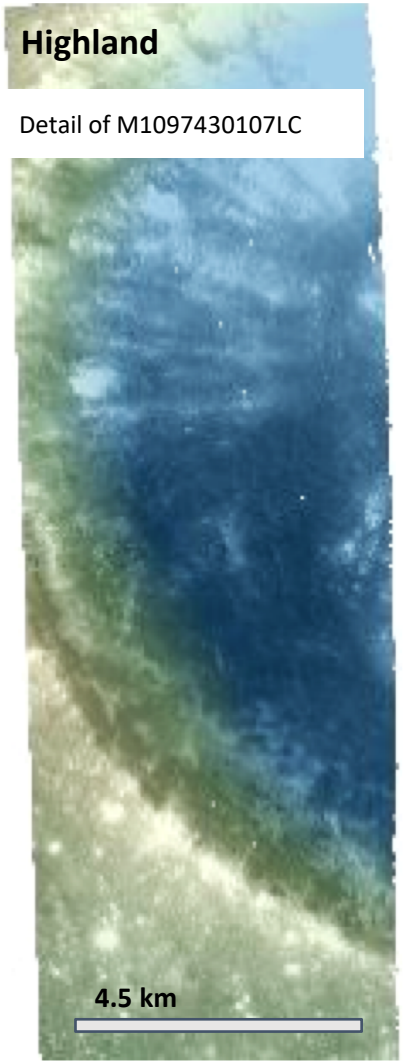
Highland
Detail of M1097430107LC
4.5 km

Internal friction angle (Φ)

Values for Φ are reported in the literature ranging from 13 to 50° (Melosh, 2011)

We measured the angle of repose of dry granular flows to refine Φ on local scales:

Region	Φ
Pyroclastic	31°
Highland & SP	30°
Mare	28°
PSR	29°

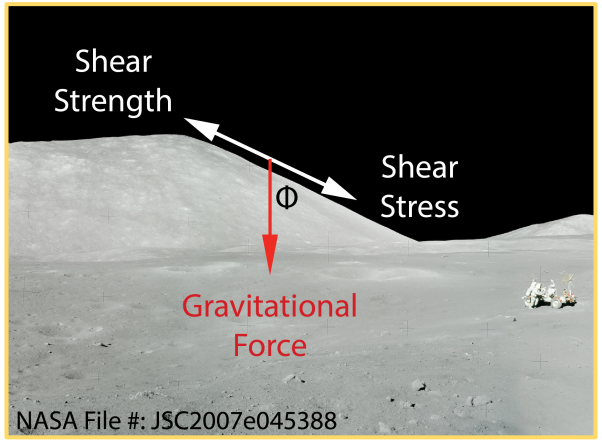

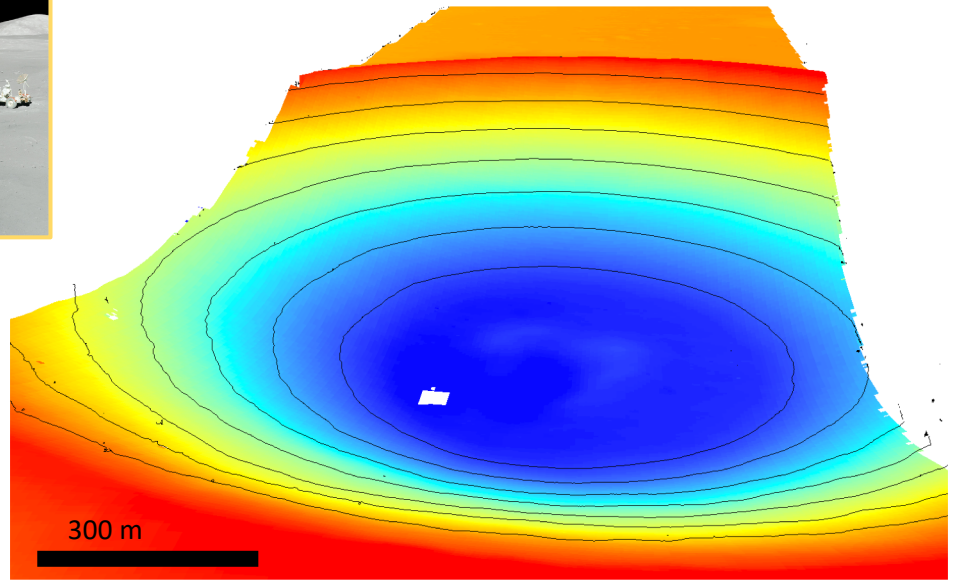

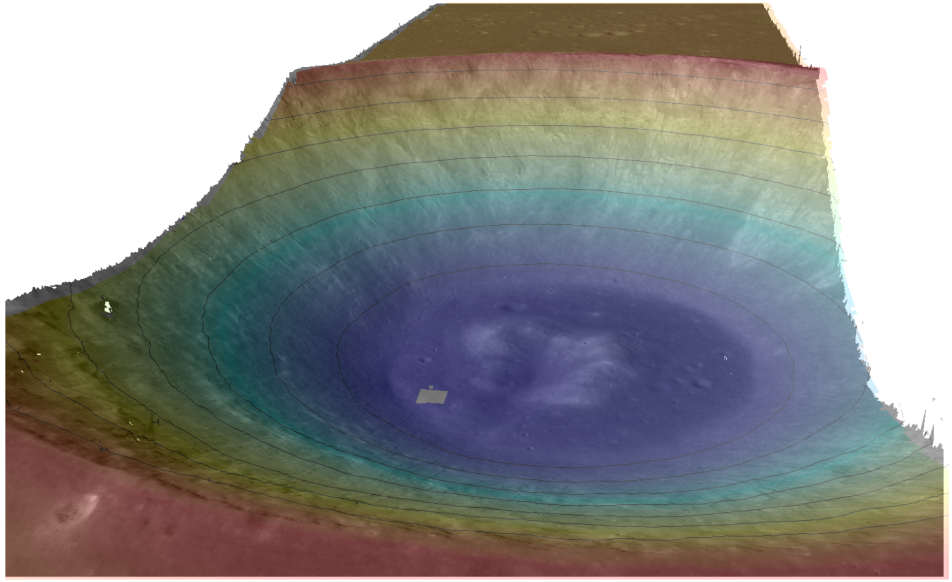

Detail of M1162383484RC

Imagery

Lunar Reconnaissance Orbiter images are used to search for boulders with tracks

→ Selected images have spatial resolutions of **0.38 to 1.27 m/pix**

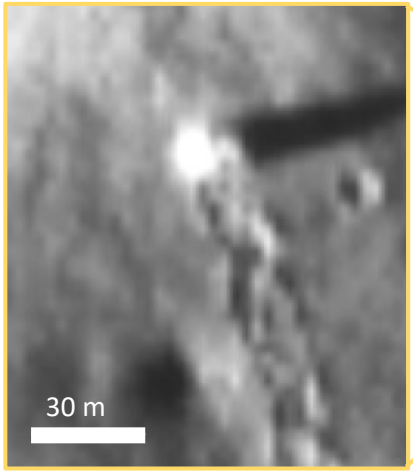

1967

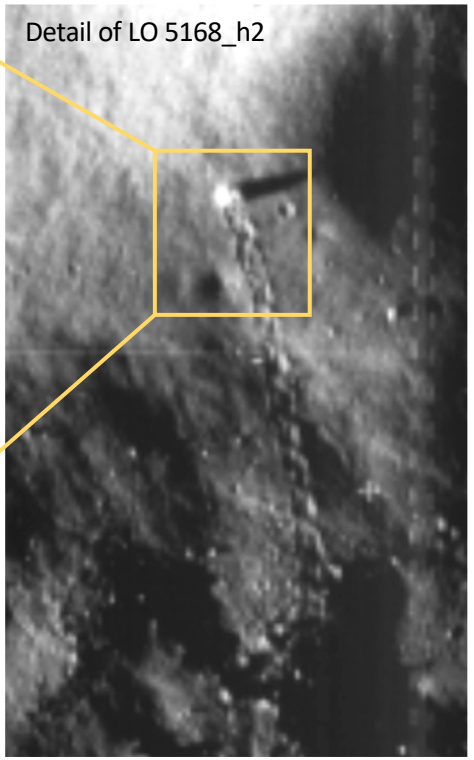

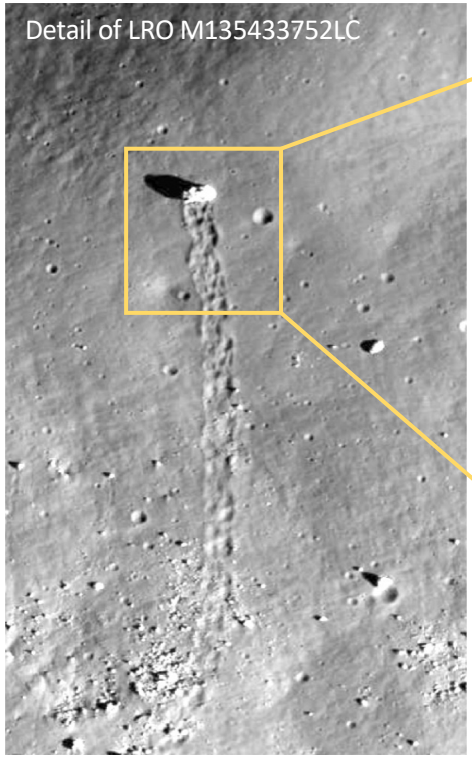

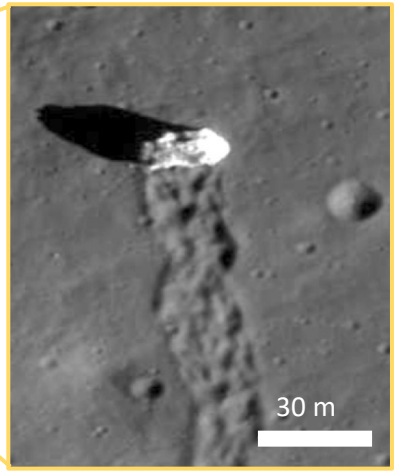

2013

Results of quantitative analysis

Bearing capacity as function of **depth** and **slope**:

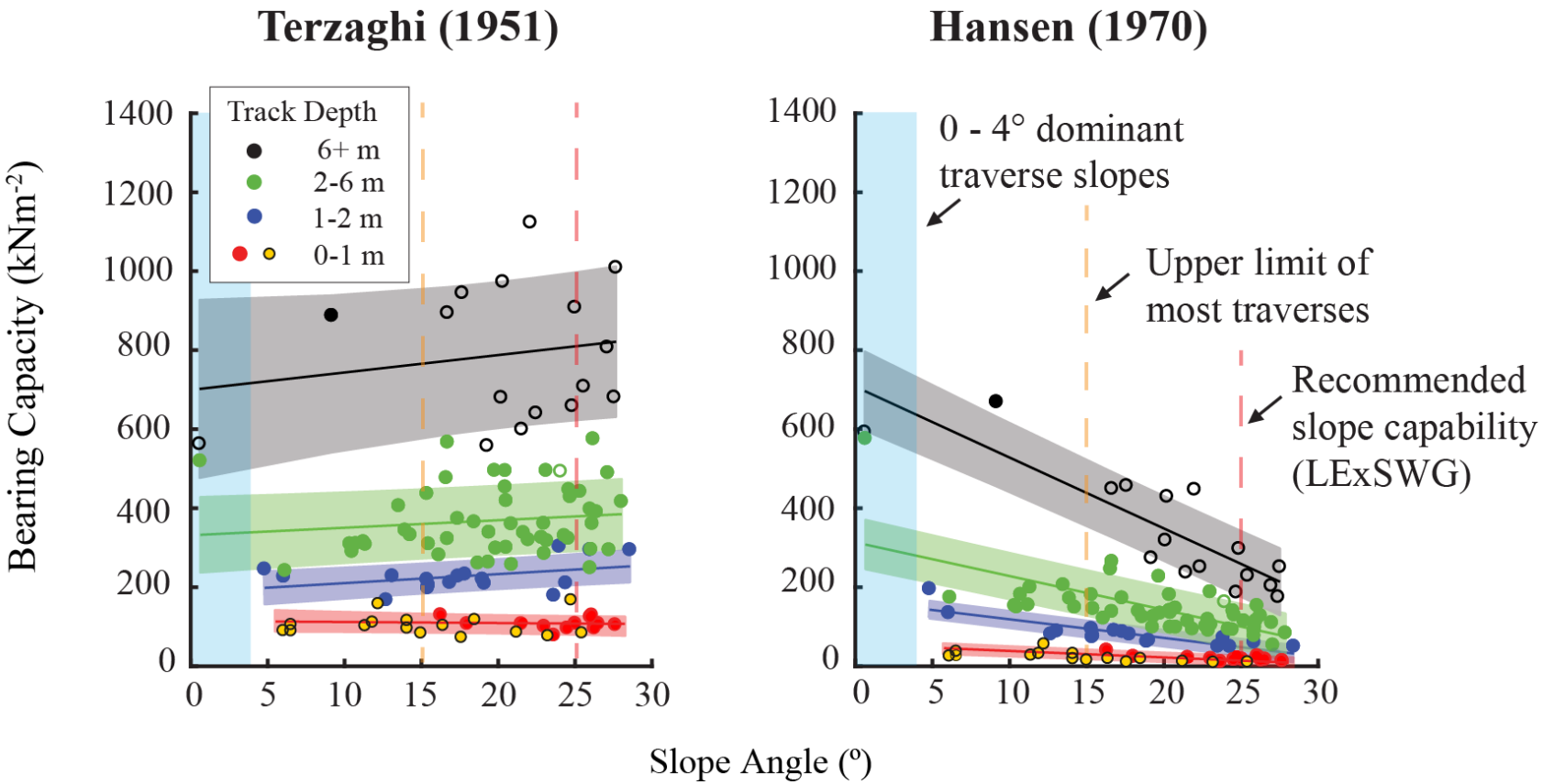

Comparison to Earth

- PSR data is skewed as a result of only shallow tracks
- Bearing capacities are equivalent to medium dense sand
- Bearing Capacity at LPDs and PSRs are statistically higher at shallow depths

[14]

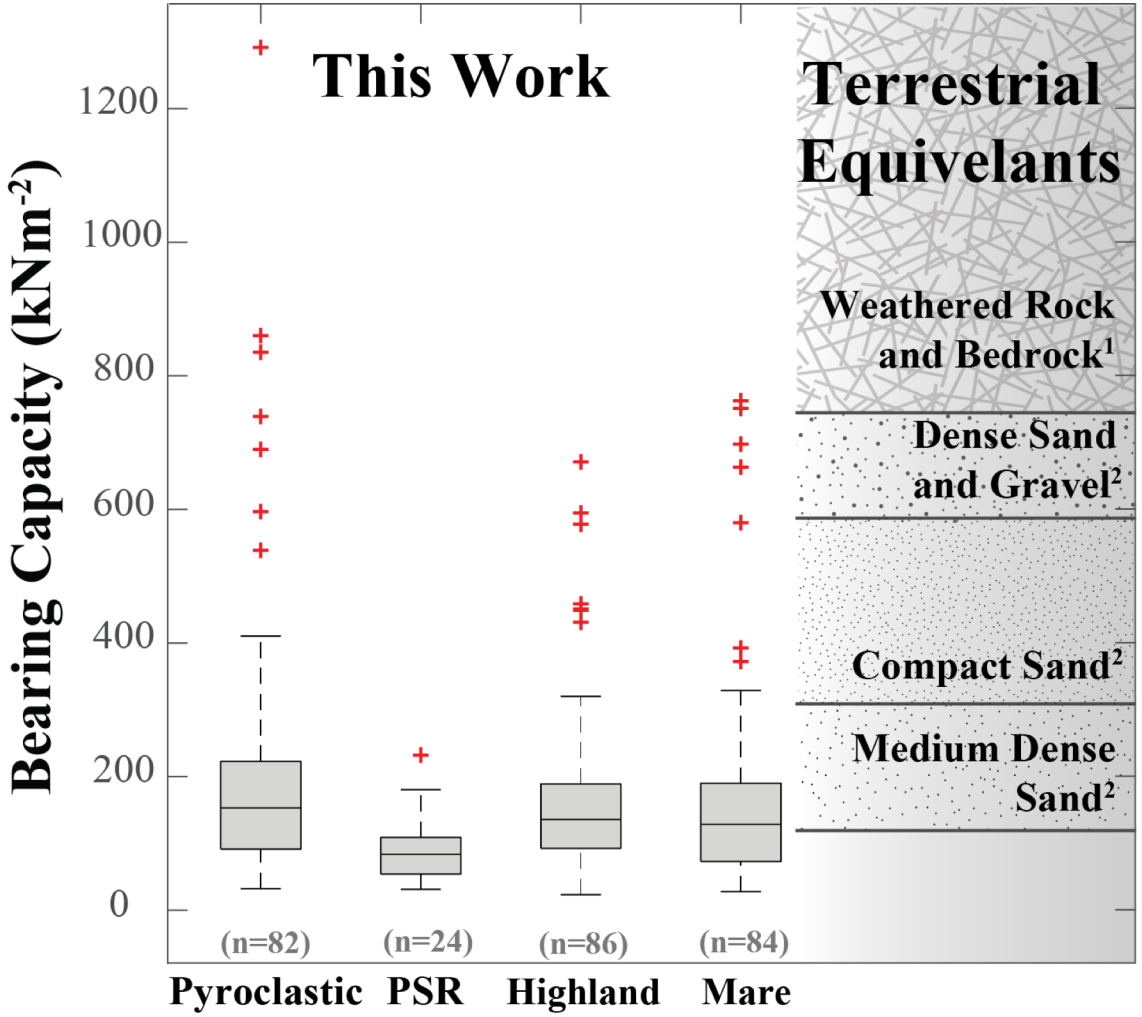

Application of this work

Bearing capacity estimate can be used to assess technical specifications of rovers that potentially are to traverse LPDs in the future:

➡ for example the Lunar South Pole

and to estimate "worst case" wheel sinkage scenarios for PSRs

➡ soil at ~10 cm depth appears able to bear high loads

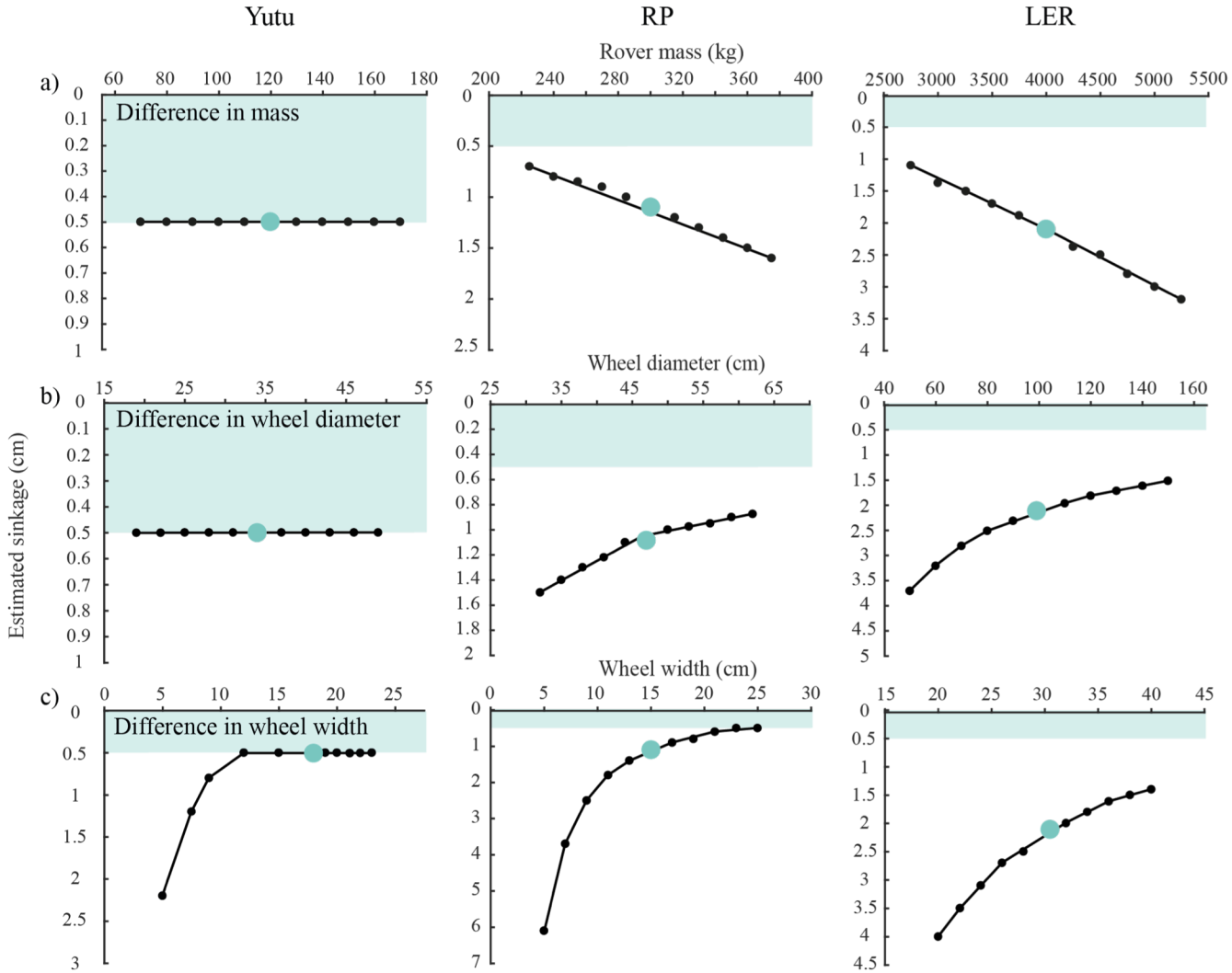

Excessive boulder track depth

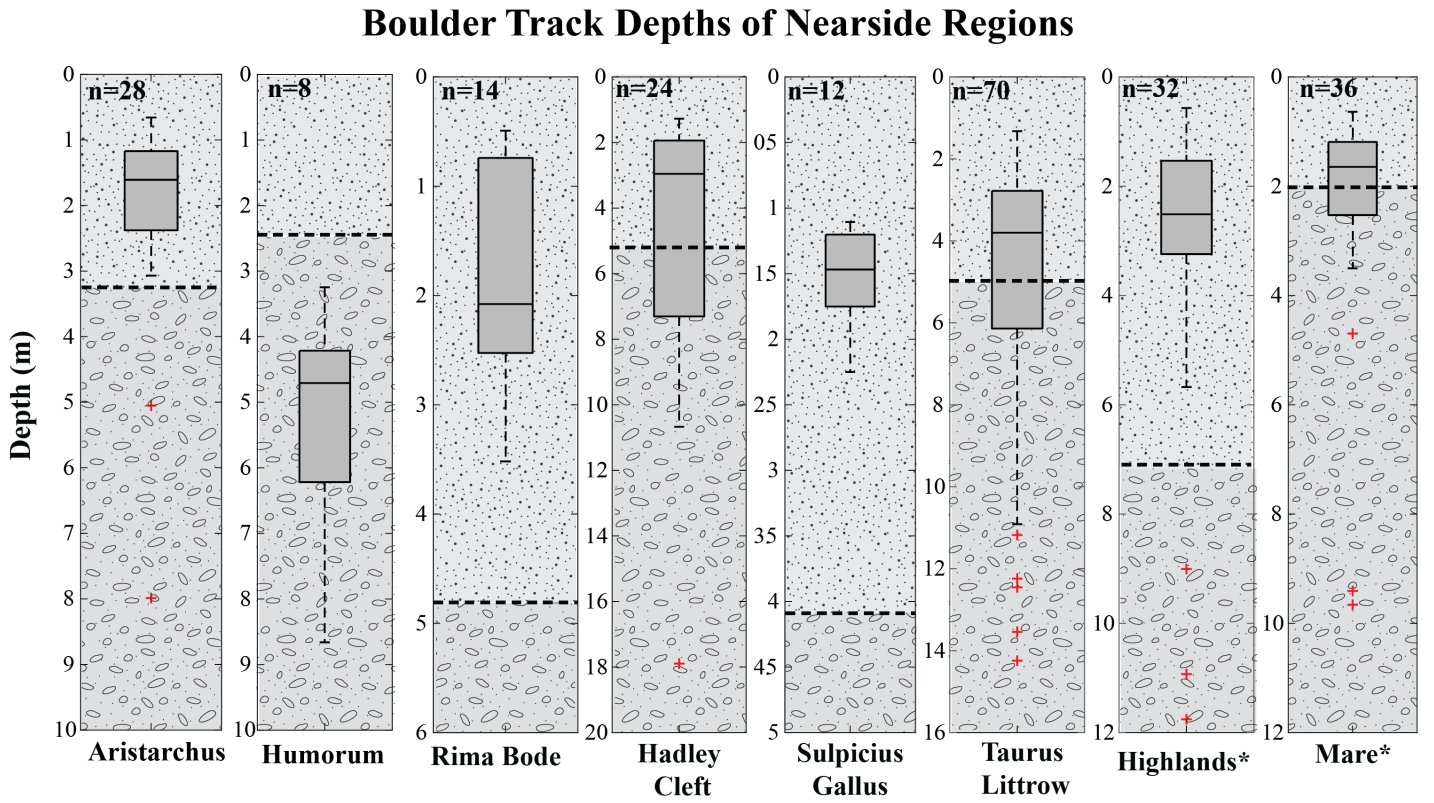

Bart et al., 2011 – Small crater morphology
Fa and Jin, 2010 – Multi-channel brightness temperature inversion
Oberbeck and Quaide, 1968 – Crater morphology
Shuratov anf Bondarenko, 2011 – Radar and optical model

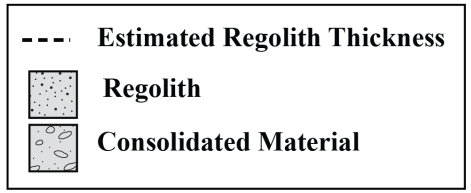

Lunar soil mechanics is important – and not completely understood

Example: Apollo 15 LRV and crew tracks illustrate changes of soil properties on small local scales

→ how can Artemis & CLPS missions help to advance our knowledge?

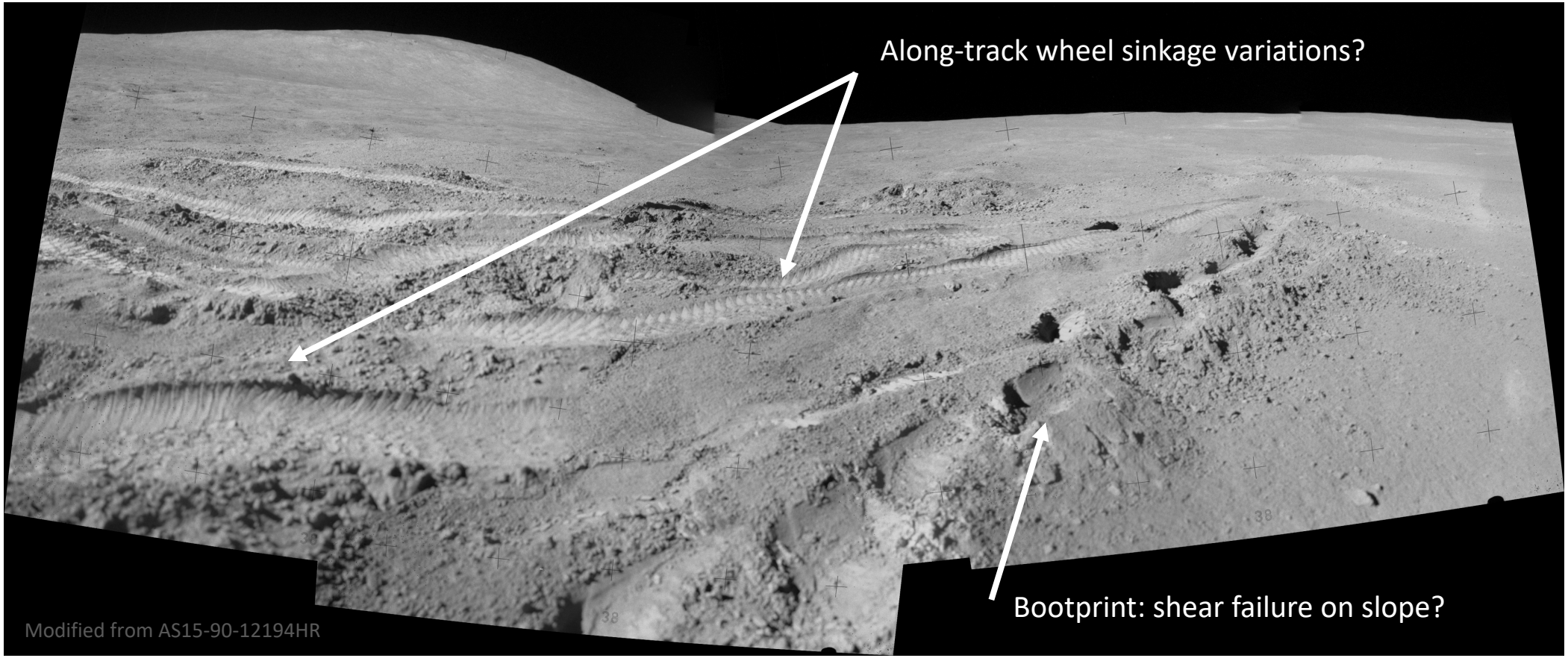

Lunar soil mechanics is important – and not completely understood

Example: Apollo 15 LRV and crew tracks illustrate changes of soil properties on small local scales
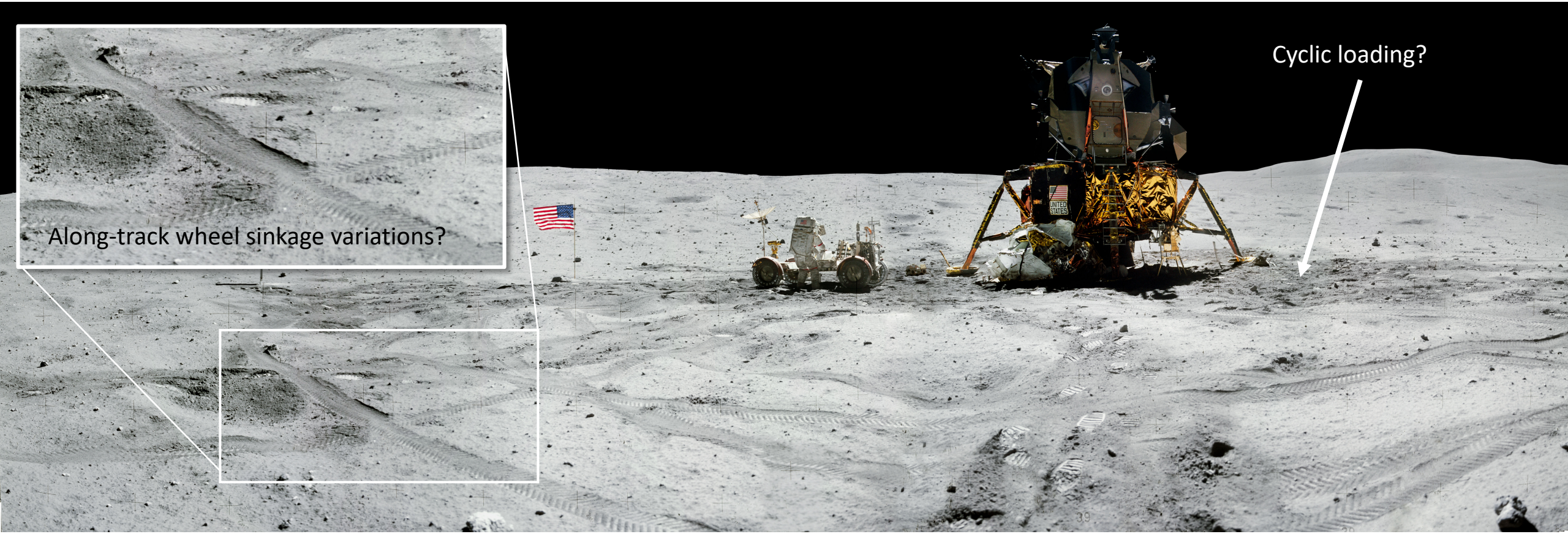
→ how can Artemis & CLPS missions help to advance our knowledge?